

# Elucidation of secondary structures of peptides using high resolution NMR

L. Gomathi\* and S. Subramanian

Regional Sophisticated Instrumentation Centre and Department of Chemistry, Indian Institute of Technology, Madras 600 036, India

\*Present address: Molecular Biophysics Unit, Indian Institute of Science, Bangalore 560 012, India

**High resolution two dimensional NMR spectroscopy has become one of the important tools in the elucidation of three dimensional solution structure of fair-sized biomolecules. In this article we summarize the application of 2D NMR techniques to unravel the structure of small proteins and peptides. The basic theme is the systematic identification of the small number of secondary structural motifs such as  $\alpha$ -helices,  $\beta$ -sheets and  $\beta$ -turns present in polypeptides using their through bond and through space fingerprints in the 2D NMR correlation maps. The method is illustrated using a 32-residue peptide which corresponds to a calcium-binding domain in the protein calmodulin.**

AMONG the various spectroscopic methods that are employed in the elucidation of the three-dimensional structure of large biomolecules such as infrared<sup>1</sup> (IR), Raman<sup>2</sup>, fluorescence<sup>3</sup>, circular dichroism (CD)<sup>4</sup> and nuclear magnetic resonance spectroscopy<sup>5-9</sup>, only NMR has become one of the most sought after techniques because of its several unique capabilities. The NMR technique which started off as a physicists' tool for measuring magnetic moments of nuclei in the fifties, today finds immense use in the biological sciences and diagnostic medicine<sup>10-13</sup>. Because of its power to reveal information on the three-dimensional conformation of large molecules in solution, NMR has become a complementary technique to X-ray crystallography. For X-ray crystallography, however, one needs single crystals of optimal size. In contrast, NMR can give information on the macromolecules even when these *tumble freely* in solution, and this has made it an important technique for the understanding of structure activity correlation in biomolecules. This is very useful since many bioactive proteins and sugars are rather difficult to crystallize. Good structural correspondence between X-ray and NMR results has been obtained in a number of globular proteins<sup>14-16</sup>, although instances are known where significant differences have been noted<sup>17,18</sup>. Another advantage of the NMR technique is that biomolecules can be studied at a simulated environment characterized by a specific pH, temperature, presence of ionic substances, etc. so that one is actually addressing the sample in physiological environment. Coupled with theoretical modelling<sup>19-23</sup> the NMR technique has provided us with a wealth of information on

protein folding<sup>24,25</sup>, denaturation<sup>26,27</sup>, intermolecular interactions<sup>28,29</sup>, etc. It is now well established that the activity of a biomolecule critically depends on its three-dimensional conformation<sup>30,31</sup>. It is known that the secondary and tertiary structures are dependent on the solvent medium, temperature, pH, presence of ions, etc. One of the major areas of research endeavour in molecular biology is 'protein folding', which is a fascinating and intriguing subject. Since the biological activity of proteins and polypeptides depends critically on the topography of the molecule apart from polarity and hydrogen bonding complementarity, it is important to get a first hand knowledge of the stereochemistry of the active site before one can start understanding biological (enzymatic) catalytic processes. This is because a transmembrane protein for example, may adopt different conformation as it traverses through the lipid membrane from the extracellular or intracellular region. It is also known that many of the enzyme proteins, which get activated only in the presence of certain metals, have different structures in the metal-bound and metal-free state. A myriad of one and two-dimensional (even higher dimensional) pulsed NMR techniques have been developed in the recent past<sup>32-34</sup>. The multi-dimensional techniques<sup>35-37</sup> in particular, have helped in the increase in resolution needed for studying large biomolecules, by spreading the frequency in more than one dimension. In this process these methods also establish unique through-bond and through-space connectivities. With the current limit of supercon magnet reaching 750 MHz for <sup>1</sup>H, biomolecules up to a molecular weight of 20 kD can be studied.

Compared to X-ray in which the position of heavy atoms is determined around 2 Å resolution, in NMR distances between 2 Å and 5 Å unit can be resolved. The quantification is rather difficult due to possible motional effects leading only to an *average* distance information. In spite of this incomplete determination of internuclear distances, three-dimensional structures obtained from NMR agree well with the corresponding crystal structures, although significant differences between solution and crystal structures have been observed in many instances. The reason for the success of the NMR method is that the three-dimensional structures of proteins are governed by the general principles

of organization in which a few limited secondary structural motifs play an important role. NMR is uniquely adopted to detect the presence of these secondary structures through NOE (*vide infra*). In fact, the detection of a very long range interaction (through space connectivity between residues far apart in the sequence) reveals specific folding of the chain to organize the secondary structures. Normally the distances are estimated by comparing the NOE cross peak intensities from a 2D NOESY spectrum<sup>8</sup>. The  $\langle r^{-6} \rangle$  dependence of the cross peak intensity will greatly reduce the relative error in the estimation of the distances which is six times lower compared to that of intensities<sup>37</sup>.

In this article we describe the use of 2D NMR techniques in the elucidation of the three-dimensional structures of polypeptides. A brief description of the methods involved in the structural elucidation of peptides is illustrated by high resolution NMR studies on a synthetic 32-residue peptide corresponding to the first calcium-binding site of the protein calmodulin.

The severe overlap of resonances places an upper limit of  $\approx 10$  kD on the molecular weight of peptides that can be studied by 2D NMR. As the molecular weight increases, further spectral simplification would require adopting 3D techniques, which improve the resolution. Often site selective isotopic substitution can enormously simplify the interpretation of spectra<sup>38,39</sup>. If the protein aggregates in solution, difficulties arise due to the broadening of the lines. A minimum of 1–2 mM of the protein itself is required to get the optimal S/N ratio in the spectrum. Most of the strategies developed for structural elucidation of proteins are also applicable to polypeptides.

## 2D NMR spectroscopy

In high resolution NMR, two major parameters, the chemical shifts and the scalar coupling constants, are needed to characterize a molecule. These give information as to the nature of the functional groups and the coupling patterns in the molecule. In addition, the nuclear Overhauser effect provides information regarding the spatial proximity of non-bonded nuclei. A complete information on the spin pattern and the through space connectivities of a molecule, should in principle, lead to the elucidation of the three-dimensional structure. However, as the molecular weight increases, the spectrum becomes complex due to severe overlap of spectral features. Therefore using 1D NMR spectroscopy, unequivocal evaluation of the spectral parameters is difficult. This becomes even more formidable when one addresses the problem of fair sized biomolecules. Methods have therefore been developed to increase the resolution of the spectrum, by spreading the same into a second dimension and in some cases even to a third dimension. The idea of a

2D strategy in NMR experiment was first suggested by Jeener<sup>40</sup>. Later various groups contributed to the development of a number of 2D techniques<sup>32,41–49</sup>.

The normal 1D NMR spectrum (whether CW or FT) is a 2D representation with one axis representing the chemical shift and the second axis, the intensity. A 2D spectrum consists of two axes representing frequencies and the third axis, intensity. 2D NMR spectra are generated using time domain techniques wherein the spin system is subjected to pulses and time intervals, and typically consists of four time sectors labelled *preparation* (P), *evolution* (E), *mixing* (M) and *acquisition* (A) (Figure 1). The preparation consists of applying an rf pulse to generate non-equilibrium magnetization. The system is allowed to evolve during the evolution period,  $t_1$ , under suitably *tailored* Hamiltonians. The third period, mixing, which is not mandatory for all 2D experiments, may consist of suitable pulses for effecting magnetization transfer, cross relaxation, chemical exchange, etc. The acquisition period,  $t_2$ , during which the signals are observed, is free of pulses except in some heteronuclear situations where it may consist of decoupling of one of the spins. The total time duration from preparation to the start of acquisition should be much less than the spin-spin relaxation time of the system so that it *remembers* the previous history and retains all the phase memories.

Generally, in 2D experiments a set of 1D data are collected by systematically varying the time interval,  $t_1$ , during the evolution period. The data thus acquired at the detection period,  $S(t_1, t_2)$ , are first Fourier-transformed

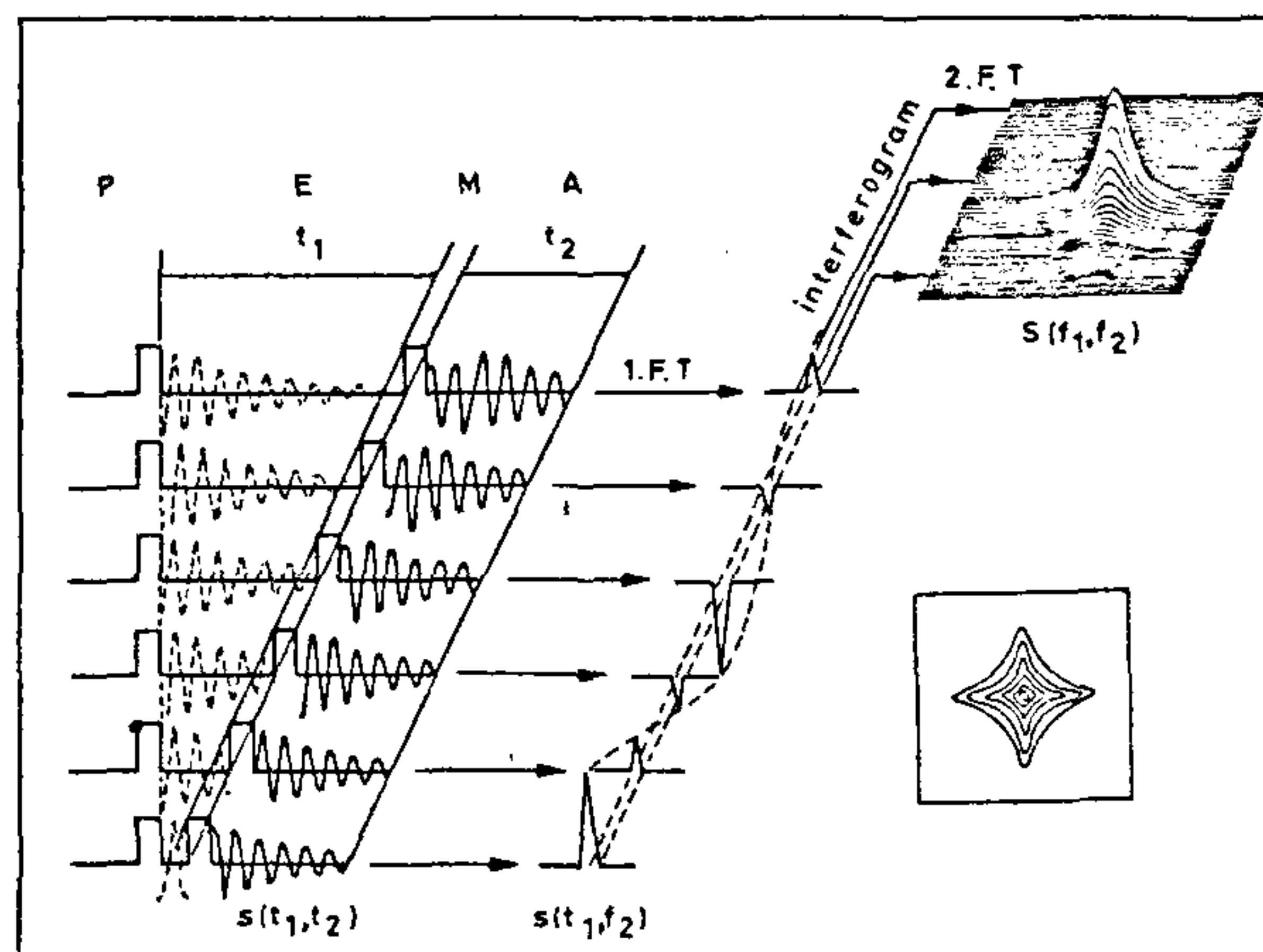


**Figure 1.** Schematic representation of 2D NMR. The four time periods are preparation (P), evolution (E), mixing (M) and acquisition (A). The signal  $S(t_1, t_2)$  is acquired as a function of two time variables  $t_1$  and  $t_2$ . FT with respect to  $t_2$  gives the interferogram  $S(t_1, f_2)$  which upon FT with respect to  $t_1$  gives the 2D spectrum  $S(f_1, f_2)$ . This can be represented either in a stack plot (inset on the top) or a contour plot (bottom inset).

along the  $t_2$  axis. The intensities of signals,  $S(t_1, F_2)$ , vary as a function of  $t_1$ , due to modulations of phase/amplitude depending upon the operative Hamiltonian. These data are then transposed and Fourier-transformed along the  $t_1$  direction, to give the normal 2D spectrum,  $S(F_1, F_2)$ . A 2D spectrum consists of three types of peaks. *Diagonal* peaks which occur at the 45° diagonal of the 2D map, correspond to the magnetization which does not undergo any transfer and was not affected by pulses, delays, etc. between the preparation and acquisition period. (A projection of the diagonal peak on either axis represents the normal spectrum.) *Off diagonal* peaks or cross peaks occurring at coordinates  $(\omega_i, \omega_j)$  with the corresponding symmetry related peak occurring at  $(\omega_j, \omega_i)$  represent connectivities either through bond or through space. Axial peaks occur at  $\omega = 0$  along the  $\omega_1$  dimension. These correspond to creation of fresh transverse magnetization signals that arise from the Zeeman magnetizations that recovered *via* spin-lattice relaxation during the  $t_1$  period and as such do not have any useful information and can be removed by suitable phase cycling. 2D spectra are either represented in a stacked mode or in a contour form. Normally contour representation is preferred, as this is more informative, where the peak intensity is proportional to the number of contours encircling the peak position (see Figure 1).

Unlike in 1D spectra, it is not normally possible to expect pure absorption mode line shapes in either or both coordinate axes of the two frequency domains. Usually, a typical 2D NMR peak has a *phase twisted* line shape, with characteristic long tails extending well beyond the position of the lines. This is because, the 2D line shape function is often a mixture of absorption and dispersion in both the dimensions. Conventionally, the practice was to plot the absolute value mode spectrum  $(u^2 + v^2)^{1/2}$  to avoid distortions in contour display. The FIDs are often weighted by suitable apodization functions<sup>42</sup> to get maximum resolution. However, absolute value mode spectrum always leads to poor resolution, hence most of the 2D sequences and the mode of acquisition have been modified in recent times so as to produce pure absorption mode line shapes in both frequency domains<sup>50</sup>.

The three most important homonuclear 2D NMR experiments are chemical shift correlation spectroscopy (COSY), total correlation spectroscopy (TOCSY) and nuclear Overhauser effect spectroscopy (NOESY). These methods involve the use of multipulse sequences, which manipulate the spins depending upon the internal Hamiltonian as well as the dynamics related to relaxation. Since nuclear spin systems are finite dimensional, the quantum mechanics of spin dynamics can be evaluated exactly<sup>32,33</sup>. In this connection it is possible to use, the Cartesian spin operators such as  $I_x, I_y, I_z$  and their products such as  $I_x S_z, I_x S_x$ , etc., as a representation of the density

operator<sup>51</sup>. It is possible to precisely describe the state of the spin state and the fate of the same during the pulse sequences and the nature of the acquired signal using the density operator formalism.

### Correlation spectroscopy

In COSY<sup>42</sup> the system is subjected to a two-pulse sequence (Figure 2). The first pulse creates transverse magnetization of all the spins. These evolve in the laboratory frame with their characteristic chemical shift ( $\delta$ ) and spin-spin coupling ( $J$ ). Those magnetizations corresponding to  $J$  coupled spins produce signed antiphase magnetization<sup>7</sup> during the evolution in  $t_1$ . The second pulse acting on these antiphase magnetizations effects a magnetization transfer coherently among coupled partners with the transfer rate being proportional to  $J/2$ . A 2D Fourier transformation of the acquired signal, therefore, produces off-diagonal peaks at coordinates

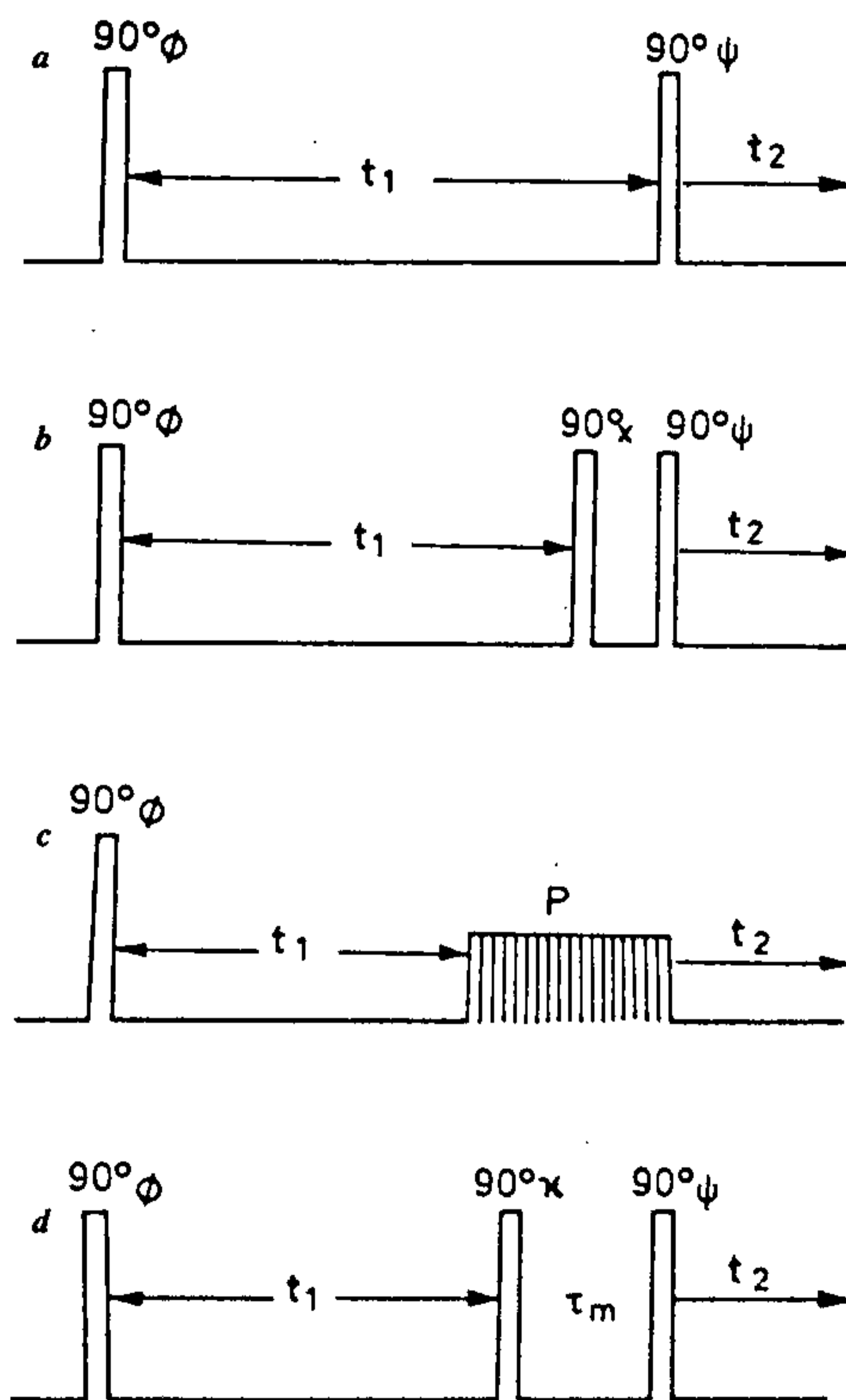


Figure 2. Pulse sequences for (a) 2D COSY, (b) 2D DQF COSY, (c) 2D TOCSY and (d) 2D NOESY. In (c) P corresponds to a composite pulse sequence for locking the magnetization in the transverse plane. In (d)  $\tau_m$  is the NOE mixing time. The phases of the various planes denoted by Greek alphabets are suitably cycled to get the desired magnetization transfer pathway.

$(\omega_i, \omega_j)$ , indicating that the two spins with chemical shifts  $\omega_i$  and  $\omega_j$  are connected through bond. COSY establishes connectivity between all directly coupled spins in the system. A detailed description of the mechanism of  $J$  connectivity and the phase cycling required to produce pure phase spectra are given in ref. 32.

In the normal COSY methodology described above, the diagonal peaks are of inphase dispersion lineshapes, they have long tails, often obscuring cross peaks close to the diagonal. Isolated equivalent spins such as methyl, isopropyl and *t*-butyl also produce exclusive diagonal peaks with long tails and often interfere with the identification of other cross peaks close to them. Since 2D COSY is essentially a means for establishing  $J$  connectivity it is possible to improve the spectrum by using double quantum filtered COSY<sup>52</sup>, DQF COSY. In this method, the second 90° pulse of COSY is replaced by a pair of 90° pulses with a very short delay in between (Figure 2). The first of these pulses generates double and higher quantum coherences only among  $J$  coupled partners, which are converted into observable single quantum coherences by the last pulse. A suitable phase cycling is used so that the magnetizations which proceed through a double quantum coherence pathway are exclusively accounted for in the  $t_2$  period. Since solvents (water, CDCl<sub>3</sub>, DMSO, acetone, benzene, etc.) and isolated spins [ $-\text{OCH}_3$ ,  $-\text{C}(\text{CH}_3)_2$ , etc.] do not possess  $J$  coupling, signals from these are eliminated from the 2D spectrum. Further, when the experiment is carried out in pure phase mode, the diagonal peaks (which now represent only spins with  $J$  coupled partners) become quite narrow because of pure absorption line shapes and enable identification of cross peaks close to the diagonal. It is to be pointed out that in going from COSY to DQF COSY, though the resolution is enhanced, there is a decrease in sensitivity since the conversion from single quantum to double quantum and back to single quantum leads to loss of magnetization in both conversions by the creation of zero quantum and  $zz$  magnetizations<sup>53</sup>.

### Total correlation spectroscopy

To establish the sequential  $J$  connectivity in a molecule, an extension of COSY is used which relies on successive relay of magnetization between spins in a network. It can be shown using density operator method, just as a single 90° pulse following a preparation pulse can transfer magnetization between directly coupled partners, further evolution followed by a third pulse will transfer magnetization between spins having a common coupling partner. Such a strategy is called relayed COSY<sup>54,55</sup>, and will establish the connectivity between spins having common coupling partners. A further extension of the relayed COSY which establishes complete connectivity

among spins in a consecutive network of coupled spins is known as total correlation spectroscopy (TOCSY)<sup>56</sup> or Homonuclear Hartmann Hahn spectroscopy<sup>57</sup> (Figure 2). In this method, after the creation of the transverse magnetization by a first pulse the spin system is effectively locked in the transverse plane using suitable continuous or composite pulse sequences<sup>58-61</sup>. Under the circumstances, the chemical shift becomes effectively zero in the rotating frame and the spin system evolves under a strong coupling Hamiltonian, J.I.S. It can be shown that such a strong coupling Hamiltonian, depending upon the various coupling constants in the network, transfers magnetization coherently back and forth at a number of frequencies<sup>62</sup>, thereby establishing complete connectivity within the network.

### Nuclear Overhauser effect spectroscopy<sup>63-67</sup>

Through space connectivity in NMR is achieved by nuclear Overhauser effect spectroscopy. The intensity of a resonance signal in an NMR spectrum is proportional to the population difference between two energy levels of the corresponding transition and, in thermal equilibrium, is governed by Boltzmann statistics. When the equilibrium populations are disturbed (*via* rf absorption), the return to equilibrium is determined by the transition probabilities. Among the various levels in the system, the internal interactions such as chemical shift anisotropy, homo and heteronuclear dipolar coupling, nuclear electric quadrupole coupling and spin rotation interactions, are made to fluctuate due to the random Brownian motion and these bring about the transitions among the levels via radiationless processes. Among all the mechanisms that bring about the establishment of Boltzmann equilibrium, the dipole-dipole relaxation is the most important, and is almost exclusively the main cause for relaxation for protons. Under this mechanism, the transition probability depends on the strength of the local field component fluctuating at the frequency corresponding to the transition under consideration. This local field is the field at the site of a given magnetic nucleus due to the presence of other dipoles.

The sequence for 2D NOESY is given in Figure 2. The first two 90° pulses effectively invert all the magnetization to the  $-z$ -axis. The non-equilibrium Zeeman magnetization tends to reach equilibrium via spin lattice relaxation brought about by dipole-dipole interaction (NOE) as explained before. In this process magnetizations get transferred between spins at a rate proportional to  $r^{-6}$ . A third pulse applied after a delay, known as the mixing time,  $\tau_m$ , generates a 2D spectrum, where the cross peaks establish dipolar connectives; suitable phase cycling is used to get pure phase spectra. Because the efficiency of 2D NOESY depends critically on  $\omega\tau_c$ , the viscosity of the medium and hence the temperature of

measurement are the factors to be controlled, along with the optimization of  $\tau_m$ . It is the capability of the NOE effect to establish magnetization transfer among dipolar partners in solution that makes the 2D NOESY the only method that can provide distance information in solution.

### 3D structure of peptides<sup>68</sup>

Amino acids are the basic building blocks of peptides. All the amino acids, with the exception of proline, have a carboxyl and an amino group on the  $\alpha$ -C atom. The individual amino acids differ in the side chain, being either aliphatic, aromatic or heterocyclic. They are usually represented by the first three letters of their names (e.g. alanine, Ala) or in short by a one-letter code (e.g. lysine, K; phenylalanine, F; etc.). The amino acids are linked together by a peptide bond to form the polypeptide chain. The peptide bond exhibits a partial double bond character and hence the six atoms,  $C_\alpha$ -CONH- $C'_\alpha$ , that characterize the peptide moiety lie in the same plane. Thus the chain can only turn at the  $C_\alpha$  atoms around the bonds N- $C_\alpha$  and  $C_\alpha$ -C' corresponding to the dihedral angles  $\phi$  and  $\psi$ . These two dihedral angles characterize the peptide backbone structure shown in Figure 3. Pro-

teins are generally described by their primary, secondary and tertiary structures. The primary structure basically identifies the various amino acid residues in their exact sequence usually numbered from the N-terminal end. The secondary structure brings about additional stabilization of the molecule through intra- and inter-molecular hydrogen bonds leading to, surprisingly, a limited number of structural motifs such as  $\alpha$ -helix,  $\beta$ -sheet and  $\beta$ -turn. Tertiary structure is brought about by the interaction among the various secondary structural elements through electrostatic, hydrophobic, van der Waals type interactions, etc. The number of protein structures solved by NMR is increasing at a tremendous pace. The advent of supercon magnets and highly sophisticated softwares to build protein models from the NMR distance data have made this one of the most important techniques<sup>69,70</sup>.

### Identification of secondary structures by NMR

Figure 4 shows the major secondary structural elements that are found in proteins and polypeptides. Each of these structural elements has characteristic through space connectivities, identification of which is the first step in understanding the phenomenon of protein folding<sup>71,72</sup>. The characteristic folding of the polypeptide chain brings different residues in close proximity and confers the overall structure on the molecule. The quantification of internuclear distances through NOE can help in arriving at the secondary structure.

The various interproton distances that are present in a folded peptide, are generally classified as sequential, medium range and long range, depending upon the number of intervening amino acid residues. By convention, the distance between protons A and B, located in amino acid residues at position  $i$  and  $j$  is denoted by  $d_{AB}(i, j)$ . For example, the distance between the  $\alpha$  proton of the  $i$ th residue and NH proton of the  $j$ th residue is denoted as  $d_{\alpha N}(i, j)$ . Sequential distances between the backbone protons are labelled as  $d_{\alpha\alpha}(i, i+1)$  and  $d_{NN}(i, i+1)$  and those between a backbone proton and  $\beta/\gamma$  protons in the side chain that are on nearest neighbour residues are labelled as  $d_{\alpha/\beta\gamma}(i, i+1)$ . Medium range distances are the nonsequential inter-residue separation between backbone protons or between a backbone proton and a side chain proton, within a segment of five consecutive residues. Long range distances are those between backbone protons that are at least five residues apart<sup>5</sup>.

Apart from the sequential distances which characterize specific secondary and tertiary structures, the secondary structures are governed by a number of medium and long range proton-proton distances. In  $\alpha$ -helix, the amino acid residues at position  $i$  and  $i+3$  are in close proximity. The distance between NH proton of the  $i$ th residue and that of  $(i+1)$  residue is short, being  $\approx 2.8$  Å. Also, the

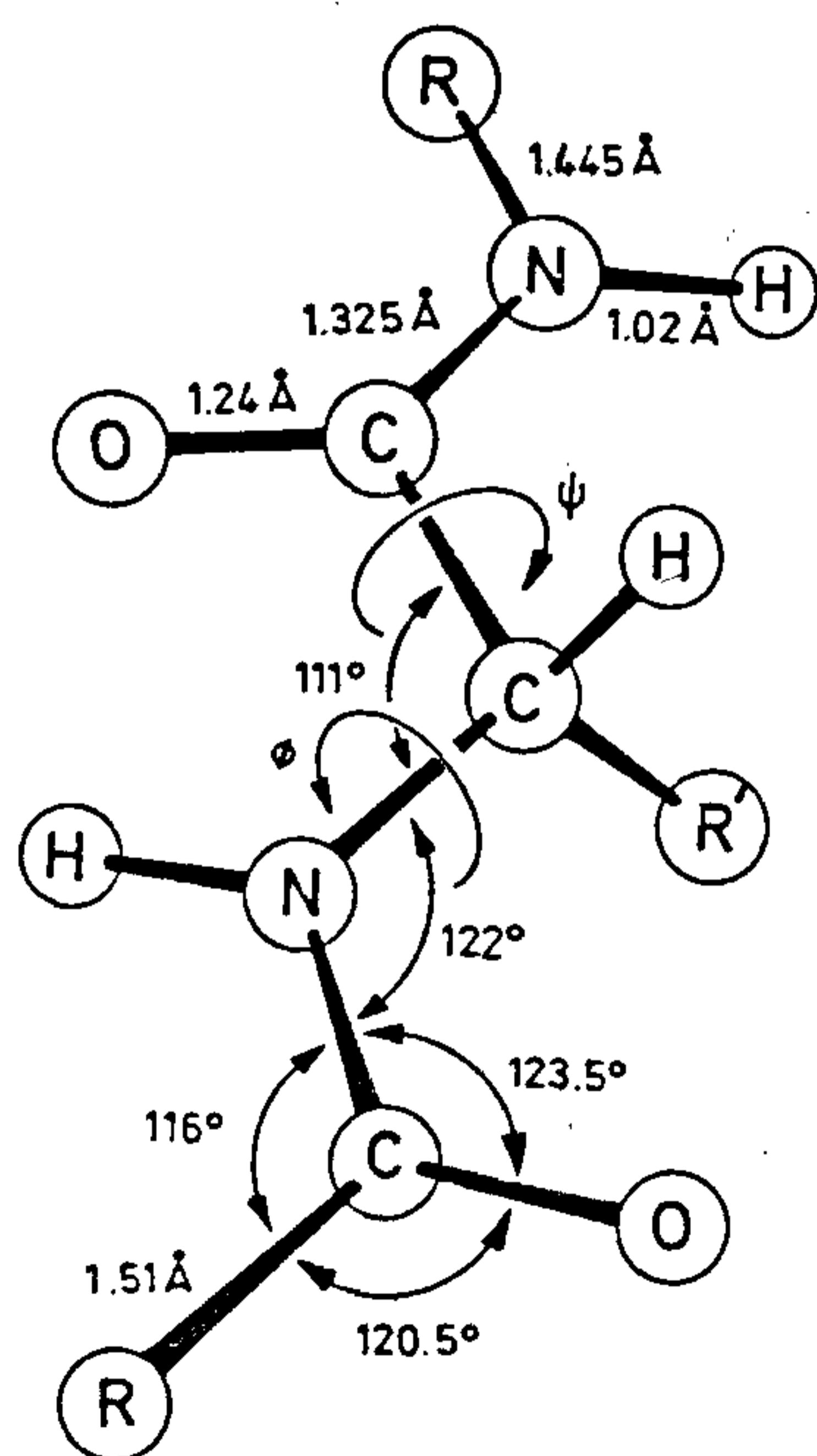


**Figure 3.** Dimensions of the peptide bond. The six atoms  $C_\alpha$ -CO-NH- $C'_\alpha$  lie in a plane. The chain has the ability to turn only at the  $C_\alpha$  atoms around the angles  $\phi$  and  $\psi$ . Here R corresponds to the continuity of the backbone while R' represents the sidechain in any residue. (Adapted from ref. 31.)

distances  $d_{\alpha N}(i, i+3)$ ,  $d_{\beta N}(i, i+1)$ ,  $d_{\alpha\beta}(i, i+3)$ , are short. The presence of NOE between the above proton pairs, especially  $d_{\alpha\beta}(i, i+3)$  and  $d_{\alpha N}(i, i+3)$  characterizes the  $\alpha$ -helix.  $\beta$ -sheets are formed when individual strands of the extended polypeptide chain come in close contact, stabilized by inter residue hydrogen bonds. These are characterized by short sequential  $d_{\alpha N}$  and interstrand  $d_{\alpha N}(i, j)$ ,  $d_{\beta N}(i, j)$  and  $d_{\alpha\alpha}(i, j)$ . The presence of inter-strand  $d_{\alpha\alpha}(i, j)$  (long range NOEs) is unique for anti-parallel  $\beta$ -sheets, whereas in parallel  $\beta$ -sheets  $d_{\alpha\alpha}(i, j)$  contacts are in the range of 4.8 Å and hence have reduced NOE. Turns are short secondary structural elements comprising four residues. These are characterized by short sequential and medium range NOEs. Table 1 summarizes the various short proton-proton distances in the secondary structural elements of polypeptides.

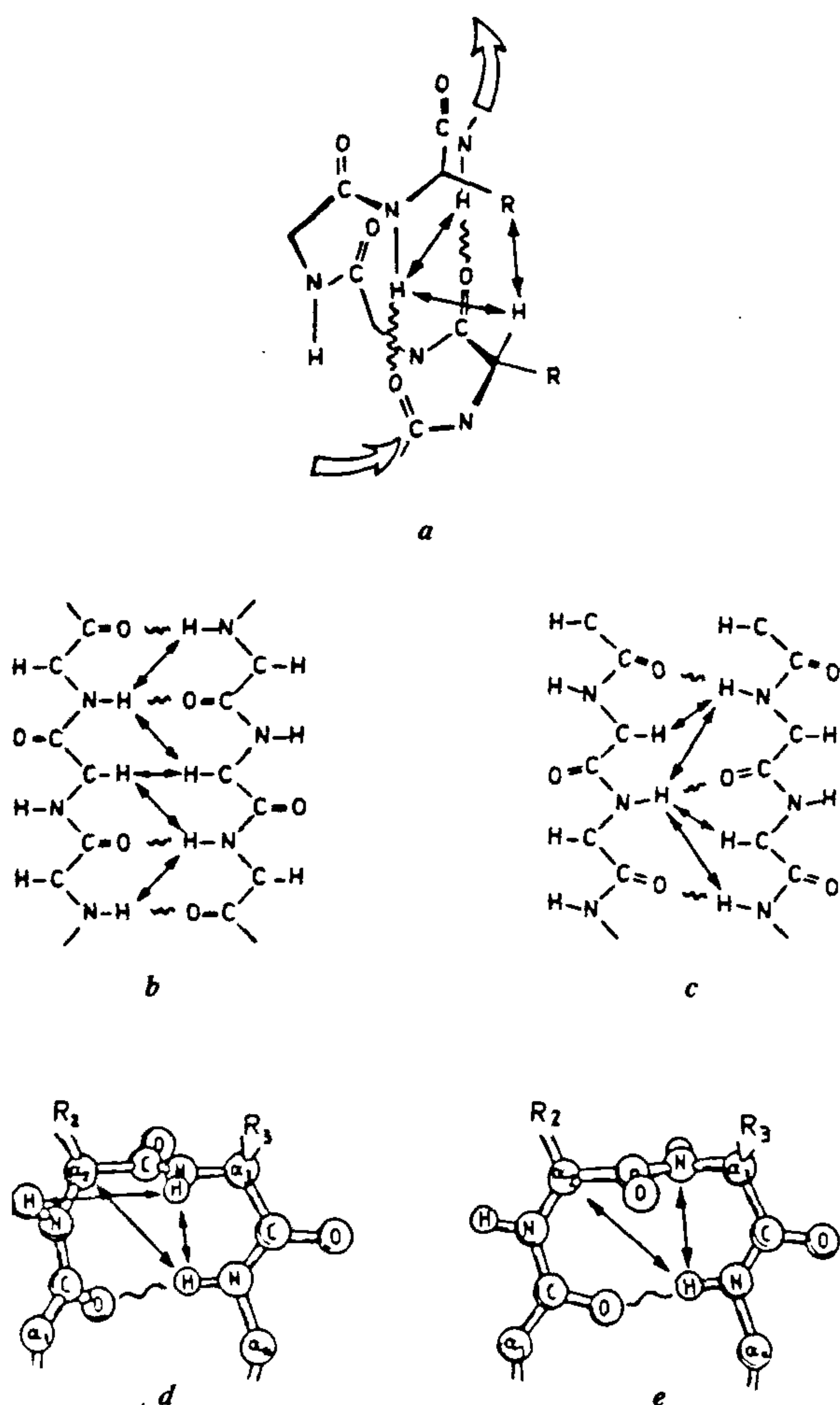


**Figure 4.** Schematic representation of the secondary structural elements in peptides: (a)  $\alpha$ -helix, (b) antiparallel  $\beta$ -sheet, (c) parallel  $\beta$ -sheet, (d)  $\beta$ -turn type-I, (e)  $\beta$ -turn type-II. Short proton-proton through space connectivities are indicated by arrows and the wavy lines correspond to hydrogen bonds. (Adapted from ref. 67.)

Besides NOE, regular secondary structures are also characterized by the three bond (H-N-C $_{\alpha}$ -H) spin-spin coupling constant ( $^3J_{\text{NH}-\alpha\text{CH}}$ ). The torsional or rotational angle around the C $_{\alpha\text{N}}$  bond ( $\phi$ ) is related to the proton-proton coupling constant that has been extensively used to probe the polypeptide conformation in solution<sup>73,74</sup>. The procedure is based on the empirical relationship between the vicinal coupling constant and the dihedral angle  $\phi$ . This is given by a Karplus type relation<sup>73</sup>

$$^3J_{\text{NH}-\alpha\text{CH}} = A \cos^2 \phi + B \cos \phi + C, \quad (1)$$

where  $A = 6.4$ ,  $B = -1.4$  and  $C = 1.9$  Hz. These have been derived using BPTI as a standard and by fitting the three bond  $J_{\text{CH}-\text{NH}}$  measured in solution and the corresponding dihedral angles derived from X-ray structure. The coupling constant is generally used for complementing the NOE distance data for the elucidation of backbone conformation of the polypeptide. The spin-spin coupling constant is normally derived from a high resolution COSY or DQF COSY spectra. It is difficult to derive an accurate estimate of this. The lines in both the above mentioned 2D techniques, appear as antiphase absorption peaks and when the line width becomes of the order of the coupling constant, the experimental  $J$  is an overestimate of the actual  $J$  (ref. 75).

The measured NOE as well as  $J$  cannot be interpreted uniquely unless it is known that the structure corresponds to a single conformer. When the polypeptide exists as an equilibrium of rapidly interconverting conformers, the NOE and  $J$  are the weighted average of the distances  $r_i^{-6}$  and dihedral angles  $\phi_i$  respectively. Since the averaging processes are nonlinearly dependent on geometry, it is often difficult to correlate the NOE and  $J$  in terms of a single conformation. When more than one conformation is possible for the molecule, the NOE derived distance<sup>8</sup> may lead to a structure, which may be energetically unfavourable<sup>9</sup>.

### Assignment of the spin systems

The information about the secondary structural content can be arrived at only when the resonances have been assigned to individual amino acids. For a small peptide, spectral overlap is minimum and useful information can be obtained from 1D NMR data itself. As the number of amino acid residues increases, the complexity of the 1D spectrum increases. This is because the NH resonances occur in the region 7–10 ppm. The appearance of all the NH residues, in a fair sized peptide, in this narrow region complicates the structural information that can be obtained from various 1D techniques. This problem is circumvented by the use of 2D NMR techniques wherein the information is spread along the second

**Table 1.** List of short proton-proton distances (Å) found in polypeptides and proteins characteristic of the typical secondary structural elements

Distance	$\alpha$ -Helix	$3_{10}$ -Helix	$\beta$	$\beta_p$	Turn I	Turn II
$d_{\alpha N}$	3.5	3.4	2.2	2.2	3.4 3.2	2.2 3.2
$d_{\alpha N}(i, i+2)$	4.4	3.8			3.6	3.3
$d_{\alpha N}(i, i+3)$	3.4	3.3			3.1-4.2	3.8-4.7
$d_{\alpha N}(i, i+4)$	4.2					
$d_{NN}$	2.8	2.6	4.3	4.2	2.6 2.4	4.5 2.4
$d_{NN}(i, i+2)$	4.2	4.1			3.8	4.3
$d_{\beta N}$	2.5-4.1	2.9-4.4	3.2-4.5	3.7-4.7	2.9-4.4 3.6-4.6	3.6-4.6 3.6-4.6
$d_{\alpha\beta}(i, i+3)$	2.5-4.4	3.1-5.1				
$d_{\alpha\alpha}$	2.5-4.4	3.1-5.1				

dimension. An improved spectral resolution and good signal to noise ratio is achieved by the use of high field NMR spectrometers.

Two different approaches are available for the complete assignment of the polypeptide chain. One method, sequential resonance assignment developed by Wuthrich<sup>5</sup>, is based on the primary structure of the polypeptide. In this method, the side chains of the various amino acid residues are assigned first and then the secondary structural elements are identified. Yet another method<sup>76,77</sup>, main chain directed strategy, is based on the secondary structure of the polypeptide moiety. In this, NOE patterns characteristic of the secondary structural elements are detected without regard to the side chain type.

### Through-bond correlation

To start with, the amino acid residues present in the system should be identified. All amino acid residues differ only in their side chains with their characteristic coupling network. Identification of the side chain spin system helps to know the type of amino acid residues present in the system.

Several 2D NMR experiments give through bond connectivities via  $J$  and these are COSY, DQF COSY<sup>78</sup>, relayed COSY and TOCSY. COSY and DQF COSY give information between directly bonded spin systems with a resolved scalar coupling. Typically in a small protein or polypeptide there would be hundreds of cross peaks. A careful analysis of COSY can give information on groups of coupled protons all present in the same residue. In other words, a given amino acid will have a basic COSY pattern quite characteristic of the residue type. For the 20 common amino acids one gets ten different COSY connectivity patterns for the aliphatic region and four for the aromatic rings (Figure 5). It is

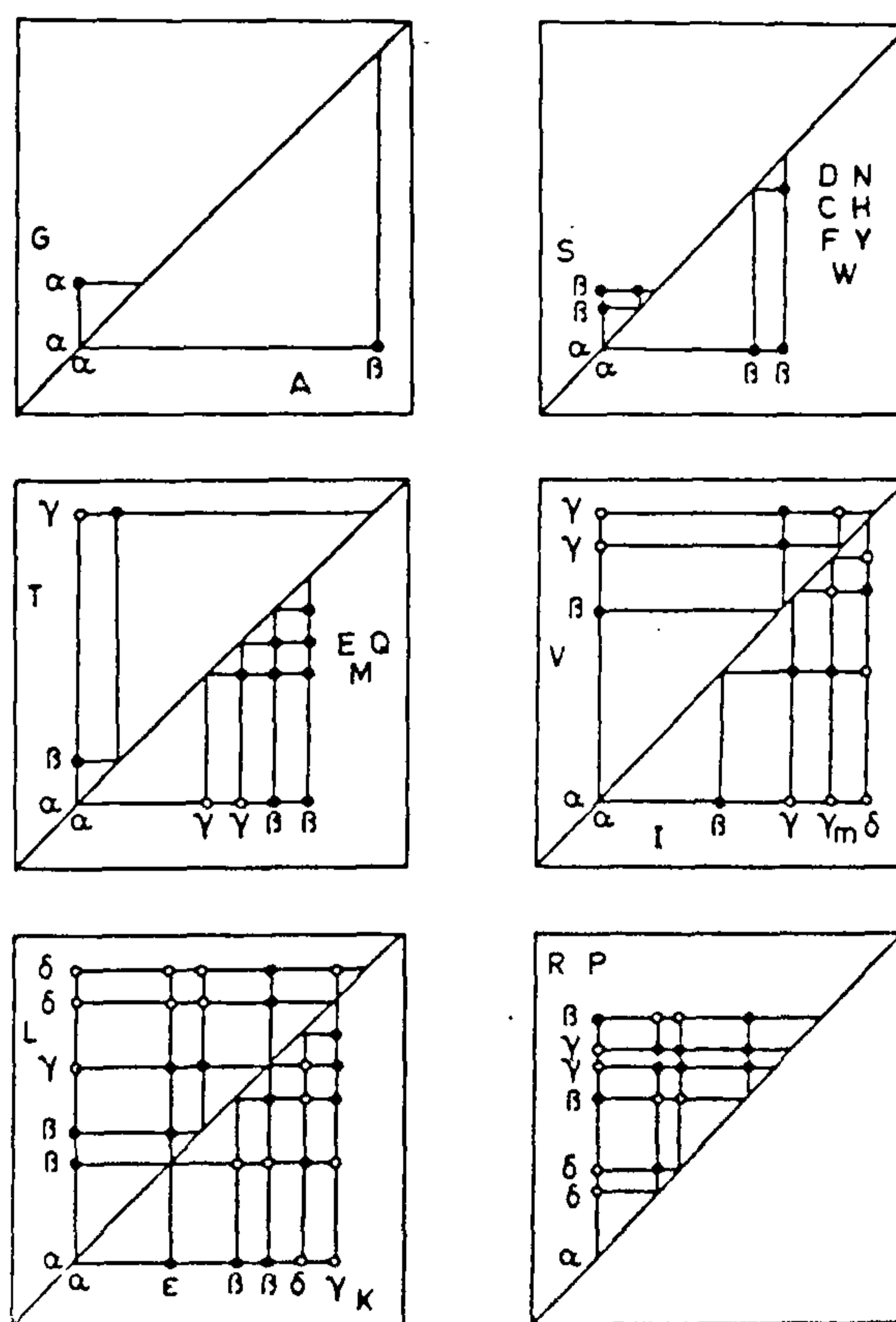


**Figure 5.** Patterns of connectivities through spin-spin coupling for the twenty naturally occurring amino acid residues. Filled circle cross peaks correspond to 2D COSY and additional connectivities by open circles occur in 2D TOCSY.

possible to identify the various residues by analysing the specific COSY connectivity patterns. For example, the residue Val has a COSY pattern consisting of  $\alpha\text{CH}$ - $\beta\text{CH}$  cross peaks and two  $\beta\text{CH}$ - $\gamma\text{CH}_3$  cross peaks. An AMX spin system, on the other hand, will produce a characteristic pattern of three cross peaks. The cross peak region between the amide protons and  $\alpha\text{CH}$  protons is the so-called finger print region, which shows a single correlation for each amino acid with the exception of glycine where the NH proton shows a correlation to two  $\alpha\text{CH}$  protons. The only residue that can be immediately identified from this finger print region is glycine. For type-specific identification of other amino acids, connectivity information between the  $\alpha\text{CH}$  and the side chain protons is necessary. Pro is the only residue that does not give any resonance in the finger print region. When any amino acid is repeated several times in the sequence, often the cross peak region may be fraught with severe overlap, especially when these are part of the random coil region of the peptide.

The amino acid residues like Gly, Ala, Val, Thr, Leu and Ile have unique spin systems. These residues are directly assigned through COSY spectrum. The amino acids, Asp, Asn, Cys, Ser and the aliphatic protons of the His, Tyr, Trp and Phe belong to AMX spin system. In this spin system,  $\alpha\text{CH}$  proton is attached to two  $\beta\text{CH}$  protons. Although in principle COSY should help in identifying various AMX patterns, severe overlap due to the presence of large number of AMX residues, impose limitation on the identification of the particular residue type. Thus, for a residue that has NH,  $\alpha\text{CH}$ ,  $\beta\text{CH}$  and  $\gamma\text{CH}$  protons, the COSY connectivities will only be manifested between NH and  $\alpha\text{CH}$ ,  $\alpha\text{CH}$  and  $\beta\text{CH}$ ; and between  $\beta\text{CH}$  and  $\gamma\text{CH}$  protons. Other set of residues like Glu, Gln, Met have  $\alpha\text{CH}$  attached to two  $\beta\text{CH}$  protons, which in turn are attached to two  $\gamma$  protons. It is difficult to assign the side chain resonances of the long side chain amino residues, like Lys, due to spectral overlap. This difficulty in most instances can be resolved by supplementing COSY data with relayed COSY or TOCSY data. A typical relay pathway is from NH- $\alpha\text{CH}$  to  $\beta$  proton with larger  $\alpha\text{CH}$ - $\beta\text{CH}$  coupling and from there to  $\gamma$  and  $\delta$  protons. In principle, therefore, TOCSY permits the correlation of all protons within a given coupling network. TOCSY with optimized mixing time, enables the complete identification of all the different amino acids, by establishing connectivity from the NH proton down to the last side chain protons. The exception is for ring protons of Phe and His residues where there is no  $J$  coupling between  $\beta$  protons and ring protons. TOCSY experiments can resolve ambiguities arising from coincident chemical shifts of the side chain protons. TOCSY is also known to be more sensitive than COSY and can offer better resolution. TOCSY patterns are also included in Figure 5.

In situations where degeneracy or near degeneracy of two resonances occur, multiple quantum spectroscopy will be useful. For example, a stringent test for distinguishing AMX spin systems from those of long side chains is that the  $\beta\text{CH}$ - $\beta\text{CH}$  cross peak of an AMX systems will be completely suppressed in four quantum filtered COSY<sup>54</sup>. Similar multiple quantum strategies can be used to resolve ambiguities in addition to simplifying the complexity of the finger print region.

### *Through space correlation*

After the identification of the resonances corresponding to the individual residues, it is necessary to identify every amino acid not only by its type but also by its position in the polypeptide sequence. NOESY gives information about distances between intra- and inter-residue protons within  $\sim 5 \text{ \AA}$  units. Depending upon the intensity of NOE peaks, classifying them as strong, medium and weak, one can roughly deal with three ranges of distances, namely short ( $< 2.5 \text{ \AA}$ ), medium ( $2.5\text{--}3.5 \text{ \AA}$ ) and long ( $3.5\text{--}5.0 \text{ \AA}$ ). To distinguish the different ranges of through space connectivities the NOESY experiment is often carried out at a number of mixing times. Often NOE cross peaks corresponding to larger internuclear distances do not show up at short mixing times.

With the unique spin topology, obtained from a combination of COSY and TOCSY, sequential connectivities between two residues of known type may provide a starting point in the sequence. This point usually corresponds to a dipeptide unit unique in the sequence. To avoid branching in the wrong direction it would be helpful to locate several di or tri peptide connectivities located along the backbone of the protein. Careful analysis of the NOESY peaks in the finger print region, when looking for specific patterns of short distances corresponding to the various motifs ( $\alpha$ -helix,  $\beta$ -sheet) can, in principle, help in the assignment.

At first sight the above procedure seems quite straightforward. However, the NH- $\alpha\text{CH}$  protons of  $\alpha$ -helices show little chemical shift dispersion<sup>79,80</sup>, compared to  $\beta$ -sheet structure and often only about 50% of the residues can be identified easily. For example, two overlapping NH resonances may show intra residue and sequential NH- $\alpha\text{CH}$  connectivity and it becomes difficult to distinguish which of the four cross peaks correspond to which of the amide protons.

Often changes in temperature, pH and amide proton exchange when dissolved in  $\text{D}_2\text{O}$ , can simplify some of the complications. In larger peptides and proteins, several NOE experiments have to be performed by varying the experimental conditions. As was mentioned previously the secondary structures do produce recognizable finger prints in the NOESY spectrum.  $\alpha$ -helices for example,

are characterized by a sequence of short NH–NH connectivities [ $d_{\text{NN}}(i, i+1)$ ,  $d_{\text{NN}}(i+1, i+2)$ , ...] corresponding to a repetitive distance of 2.8 Å. The NH– $\alpha$ CH distances in  $\alpha$ -helix give strong NOE cross peaks. In addition, weak inter-residue correlation between NH– $\alpha$ CH of the preceding residue  $d_{\alpha\text{N}}(i, i+1)$  and to the  $\alpha$ CH of the residue three positions earlier  $d_{\alpha\text{N}}(i, i+3)$  characterize the  $\alpha$ -helix. Other connectivities in the  $\alpha$ -helix are  $d_{\alpha\beta}(i, i+3)$ ,  $d_{\beta\text{N}}(i, i+1)$  and relatively weaker  $d_{\alpha\text{N}}(i, i+2)$ ,  $d_{\alpha\text{N}}(i, i+4)$ .

Antiparallel  $\beta$ -sheets will have, in addition to their interstrand  $\alpha$ CH– $\alpha$ CH cross peaks, intense  $d_{\alpha\text{N}}$  connectivities. Parallel  $\beta$ -sheets on the other hand, show sequential  $d_{\alpha\text{N}}$  connectivity but rather weak interstrand  $\alpha$ CH cross peaks. Figure 6 summarizes the various through space, NOE connectivities expected for typical secondary structural elements found in peptides and proteins.

A complementary information regarding secondary structure is obtained by quantitatively analysing the NH– $\alpha$ CH spin–spin coupling. Often this is done from DQF COSY spectrum with a high digital resolution in the finger print region. The Karplus relation and experimental data show that in general, this  $^3J_{\text{NH}-\alpha\text{CH}}$  is in

the range of 4–5 Hz for  $\alpha$ -helix whereas it is nearly 9 Hz for  $\beta$ -sheets. The various turns (type I, II, etc.) cannot be distinguished from  $\alpha$ -helix using this information alone.

When ambiguity arises in the total assignment of the spectrum using the 2D methods mentioned above, one can resort to additional techniques such as double labelling with  $^{13}\text{C}$  and  $^{15}\text{N}$  of specific residues in the sequence which will aid in the assignment. This is because  $^{13}\text{C}$  exhibits long range  $^2J_{\text{C-H}}$  with NH of the next residue and its own  $\alpha$ CH. Each amide  $^{15}\text{N}$  has a resolved coupling with its own hydrogen ( $^1J_{\text{N-H}}$ ) and with the  $\alpha$ CH of the preceding residue. In peptides which lie in the intermediate tumbling region ( $\omega\tau_c = 1.12$ ), NOESY fails and one has to resort to ROESY<sup>81,82</sup> as well as the above mentioned isotopic labelling methods to arrive at the 3D structure. Another useful method is to label the side chain randomly to about 75% with  $^2\text{H}$ . This leads to a substantial gain in the resolution because of the lengthening of the  $T_2$  (refs 83, 84). In addition, the improved resolution is also due to the removal of spin–spin coupling between  $\alpha$ CH and aliphatic protons. Random deuteration of the side chain leads to a gain in sensitivity in the NH–NH region of the NOESY spectrum as well, because during the mixing period of the experiment, there is a substantial reduction in the loss of magnetization due to the deuterated aliphatic chains<sup>85</sup>.

Once the assignments of coupling network and unambiguous interpretations of NOESY spectra have been accomplished, one can resort to using this information in a distance-constrained molecular modelling study<sup>86</sup>. However, a detailed description of the procedures will not be dealt with in this article. A schematic diagram for arriving at the most probable structures using the NMR-derived parameters as constraints is given in Figure 7.

In Figure 8 the overall summary of the structure determination of the biomolecules using NMR and NMR-assisted modelling studies is provided as a flow chart.

### 3D structure of a 32-residue peptide

In this last section we have taken an illustrative example from our attempts to study the 3D structure of some synthetic CaM fragments<sup>87</sup> corresponding to the various calcium-binding sites in isolation to see whether these have reasonable extent of secondary structures. The peptide chosen is labelled 1–1–1 and corresponds to the first calcium-binding site characterized by helix 1–loop 1–helix 1 corresponding to the residues 10–41 in the native CaM molecule, namely, AEFKEAFSLFDK DGDGTITTKELGTVMRSLGQ.

### Experimental

The CaM fragments were synthesized using a modified

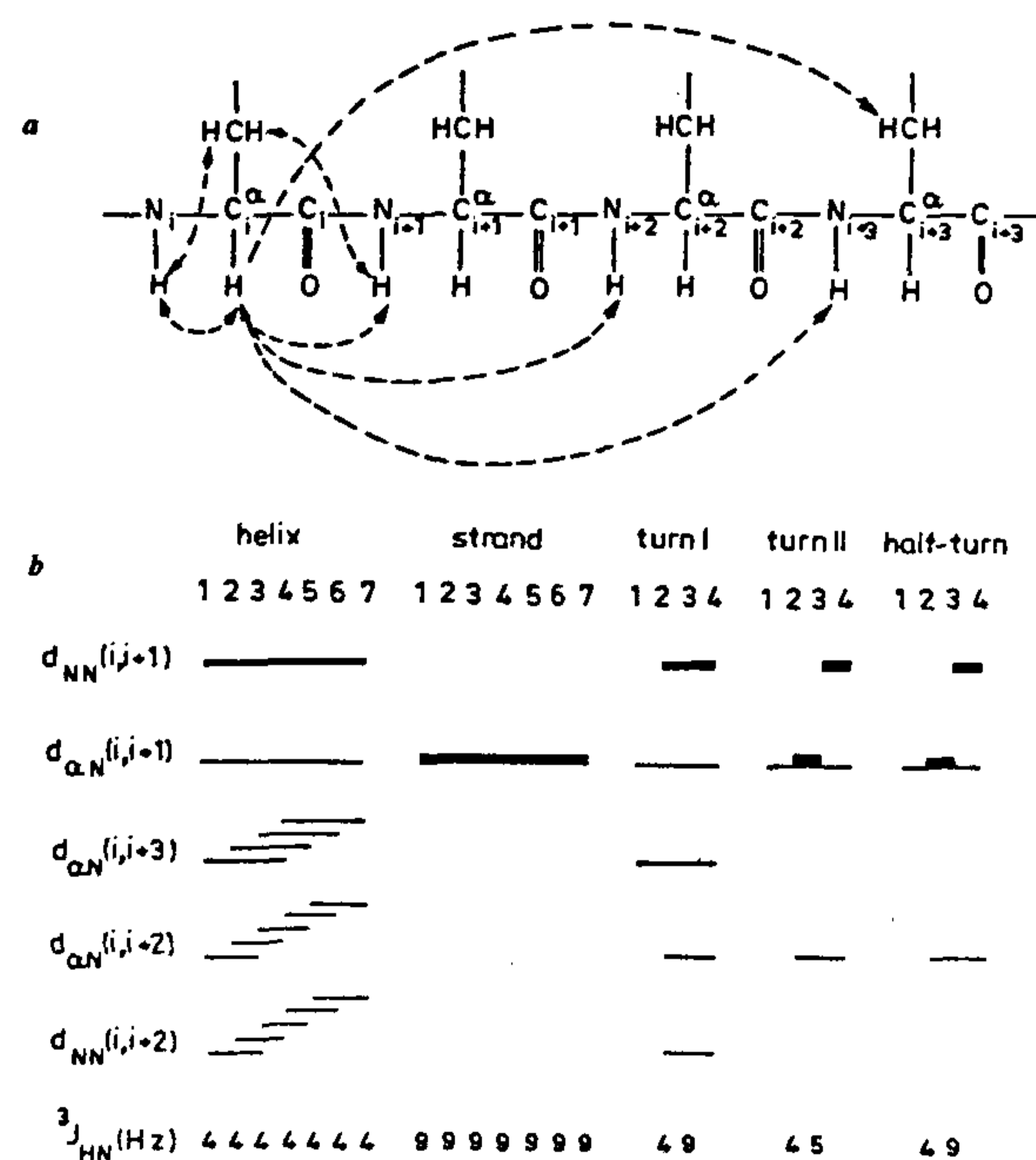


Figure 6a,b. a, Schematic representation showing through space connectivities in peptides between protons which give NOE cross peaks. b, The various through bond connectivities in typical secondary structural elements in peptides that give NOE cross peaks. The thickness of the lines corresponds to the relative intensities of the cross peaks. The bottom row contains  $^3J_{\text{NH}-\alpha\text{CH}}$  coupling constants in Hz. (Adapted from ref. 5.)

Merrifield solid phase method<sup>88</sup>. The crude peptide was purified by reverse-phase HPLC and the purity and identity was confirmed by analytical HPLC and by amino acid sequencing. NMR experiments were carried out using a JEOL GSX 400 spectrometer and a BRUKER AMX 600 spectrometer. Measurements were made at 40°C with a peptide concentration of 4–5 mM in DMSO- $d_6$ . A spectral width of ~7500 Hz was used. The residual water peak in DMSO was suppressed using a presaturation pulse of 2 s duration. 2D NMR spectra, viz. DQF COSY, TOCSY and NOESY were obtained generally with 1 K complex data points, 32 transients, 256  $t_1$  increments and were zero filled to 2 K × 2 K points. In some experiments the parameters were changed depending upon the requirements. Before Fourier transformation, the time domain signals were weighted by sine square or sine bell window functions in both dimensions. NOESY mixing times were optimized after doing several 2D experiments and a mixing time of 400 ms was found to be adequate. Similarly for the 2D TOCSY experiment a mixing time of 60 ms was used. All 2D NMR experiments were carried out in the phase sensitive mode and processed according to the procedure of States *et al.*

### Results and discussion

The analysis of NMR spectra is based on the sequential

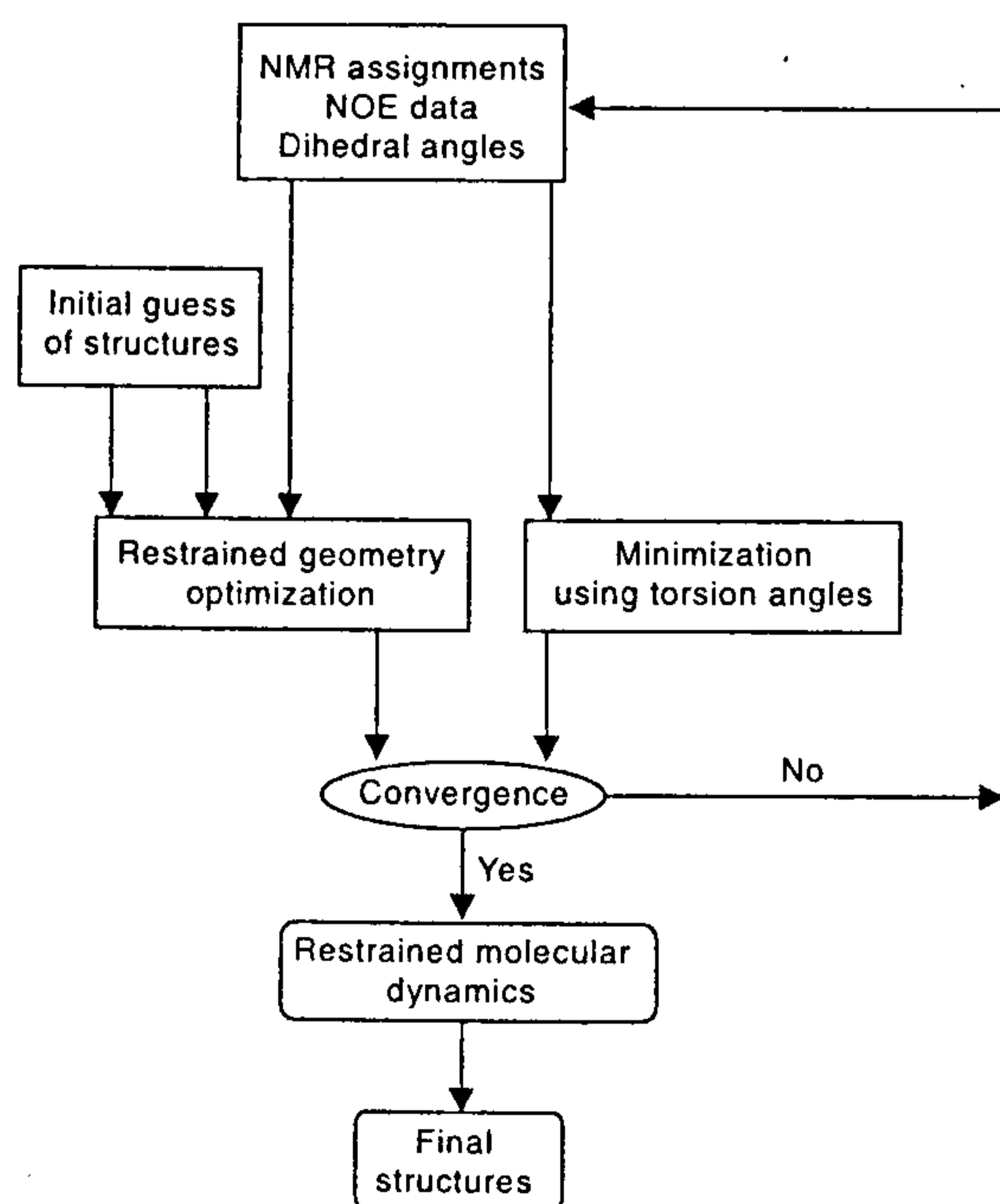


Figure 7. Flow chart for the determination of structures of peptides on the basis of NMR data.

resonance assignment procedure developed by Wüthrich *et al.*<sup>74</sup>. This is a two-stage process. The first step involves the assignment of each cross peak in the *finger print* region to a specific amino acid type. The experiments, COSY, DQF COSY and TOCSY give information about the through bond scalar coupled spin systems. Amino acid residues with unique coupling patterns could be identified clearly whereas the other cross peaks can only be assigned to more general classes of amino acid types. Complete spin system assignment depends on the resolved coupling patterns and on the topology of the spin system under consideration. In the second stage, the cross peaks are assigned to the specific amino acid residues in the peptide sequence using NOE data<sup>79</sup>.

**Analysis of the spin systems.** The peptide 1–1–1 consists of 32 amino acid residues. The DQF COSY spectrum for this peptide is shown in Figure 9a. Of the 32 residues, the finger print region clearly shows at least 22 of the NH- $\alpha$ CH connectivities. The remaining residues could not be located either due to severe overlap or

### Steps in the structure determination of peptides by NMR

1. Sequential resonance assignment:
  - (a) Use COSY, DQF COSY, TOCSY and in some cases MQ spectroscopy to assign spin systems using through bond connectivities.
  - (b) Identify the flanking residues to a given amino acid by means of NOESY utilizing short-range connectivities.
2. Explore tertiary connectivities between non-neighbour residues through long range NOEs.
3. Estimate through space distances by quantifying NOEs into categories such as weak, medium and strong so that some distance constraints can be derived that will be useful in modelling.
4. Use the DQF COSY and other versions of COSY that allow quantitative estimates of three-bond coupling constants that will be useful to arrive at backbone torsion (dihedral) angles.
5. Look for the presence of segments of sequential connectivities that would indicate the presence of helices and probably  $\beta$ -sheets.
6. Finally try to arrive at the three-dimensional structure using a combination of NOE data and torsion angles in conjunction with one or more of the following approaches.
  - (a) Molecular model building packages with NOE derived distance constraints.
  - (b) Comparison with X-ray derived structures of the same peptides or homologues.
  - (c) Restrained least squares minimization in torsion angle space.
  - (d) Restrained molecular dynamics.

Figure 8.

due to the corresponding peaks being absent in the finger print region (Figure 9b). This might be due to the very low intensity arising out of a small NH- $\alpha$ CH coupling constant or due to the large line width. Also the overlap of antiphase components in DQF COSY spectrum leads to cancellation of most of the cross peak intensity.

The peptide 1-1-1 has 12 amino acid residues with unique spin systems, 8 of AMX type and 12 long side chain residues. There are four glycines at sequence positions 14, 16, 24 and 31. Two of the glycines are identified based on their characteristic cross peaks in the COSY spectrum. One more glycine residue, with degenerate  $\alpha$ CH protons, is identified from the sequential NOE data. Two alanines at sequence positions 1 and 6 are identified from the COSY and TOCSY spectra. The assignment of the  $\alpha$ CH proton is difficult due to severe overlap. One valine and all the four threonines are assigned unambiguously from the COSY and TOCSY spectra (Figure 10a, b). The identification of Ile and Leu residues is based on the appearance of the NH- $\delta$ CH<sub>3</sub> cross peaks. Unambiguous assignment is achieved only from the analysis of NOESY spectrum. Thus out of 15 residues of this type, 11 residues are assigned unambiguously.

The only aromatic residue present in this system is phenylalanine. Two of the three Phe are identified from the possible NOE cross peaks between the aromatic ring protons and the aliphatic protons of the same residue. NH resonance of one of the Phe is missing, but its

position is identified from the NOE data. Two serines are distinguished from the aspartate residues due to the low field resonances of  $\beta$  protons. Seven out of eight residues of this type are thus identified.

The long side chain spin systems were grouped into one class partly on the basis of chemical shift values of the  $\beta$ CH protons and partly on the patterns of the  $\alpha$ CH- $\beta$ CH cross peaks which are distinct from those of the AMX spin systems. The identification of the additional resonances belonging to the spin system helps in distinguishing the type of amino acid, i.e. lysines from glutamates, methionines, etc.

**Sequential assignment.** The sequential assignment of the peptide 1-1-1 dissolved in DMSO solution is based on the analysis of NOESY spectra with a mixing time of 400 ms (Figure 11a). The unambiguous assignment of the residues valine, glycine and threonine helps in the identification of the sequence position of the other residues. Analysis of the finger print region of the NOESY spectrum helps in the assignment of the peptide segments, Phe-3-Lys-4; Asp-11-Lys-12-Asp-13-Gly-14-Asp-15; Gly-16-Thr17; Gly-24-Thr-25; Val-26-Met-27. The peak position of the Phe-3 is located on the basis

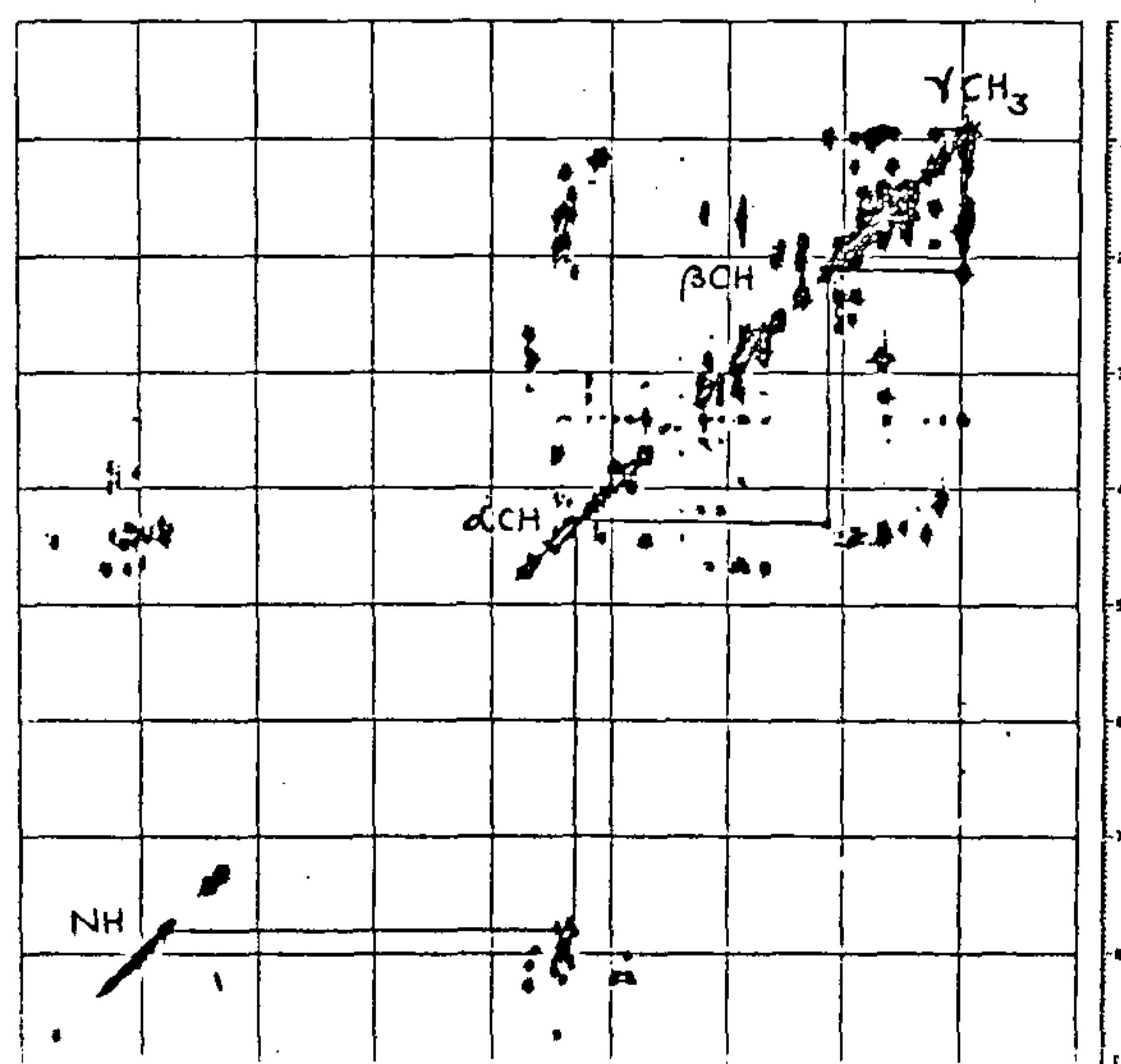


Figure 9a. 600 MHz phase sensitive DQF COSY spectrum of the peptide 1-1-1 in DMSO at 40°C. The COSY connectivities of valine are shown.

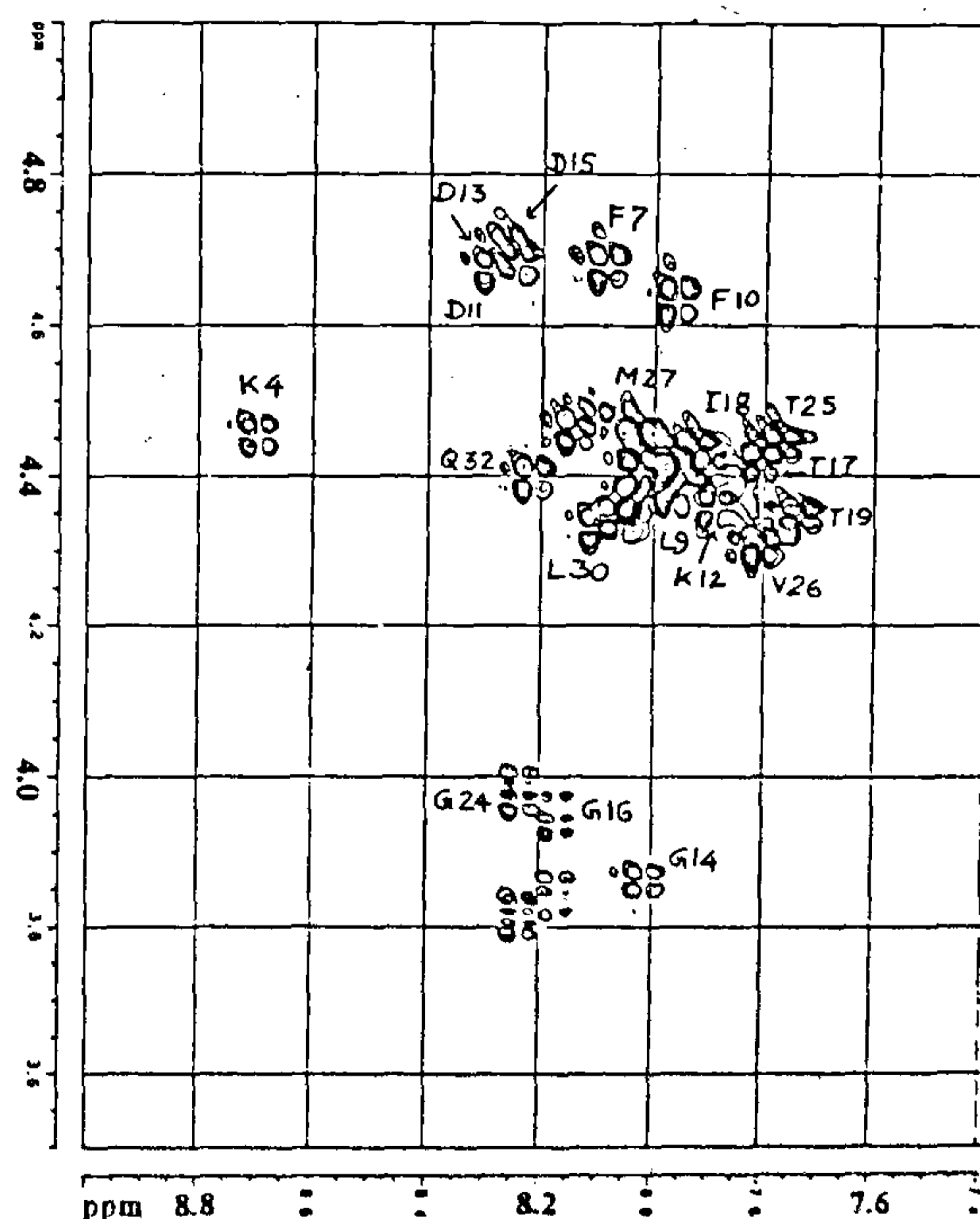


Figure 9b. 600 MHz phase sensitive DQF COSY spectrum of the peptide 1-1-1 in DMSO at 40°C, showing the expanded finger print region. The NH- $\alpha$ CH cross peaks have been labelled with the one-letter amino acid codes.

of its NOE with Lys-4. The other two phenylalanines are at positions 7 and 10. The residue at position 10 is identified on the basis of the NOE cross peak between the ring proton and the  $\gamma$ CH proton of Leu-9. Thus all

the three phenylalanines are located clearly. Analysis of the NH-NH region of the NOESY spectrum (Figure 11 *b*) confirms the sequential assignment. The residue Leu-23 is assigned based on the NH-NH cross peak between

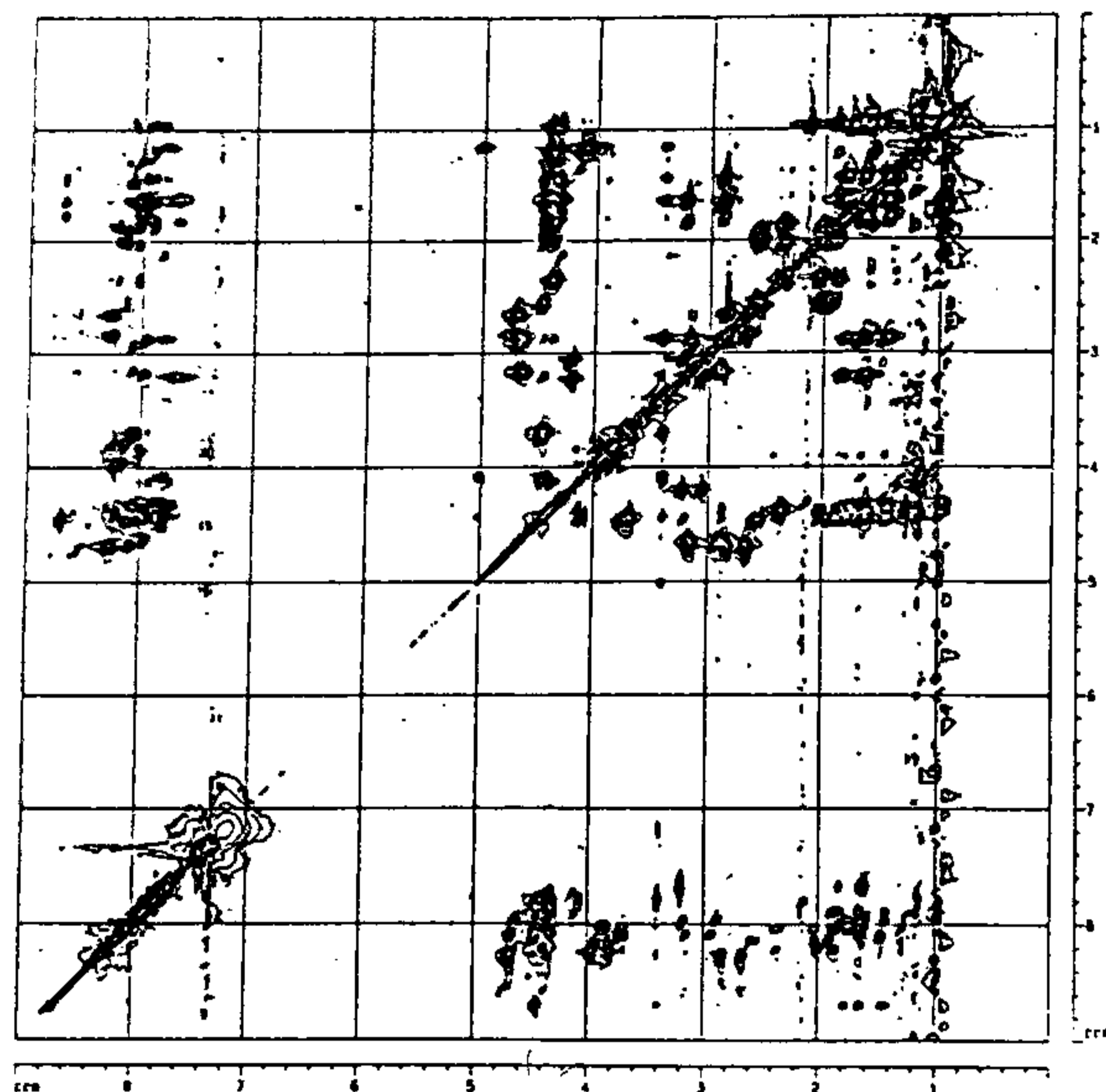


Figure 10 *a*. 600 MHz phase sensitive TOCSY spectrum of the peptide 1-1-1 in DMSO at 40°C with spin lock duration of 60 ms.

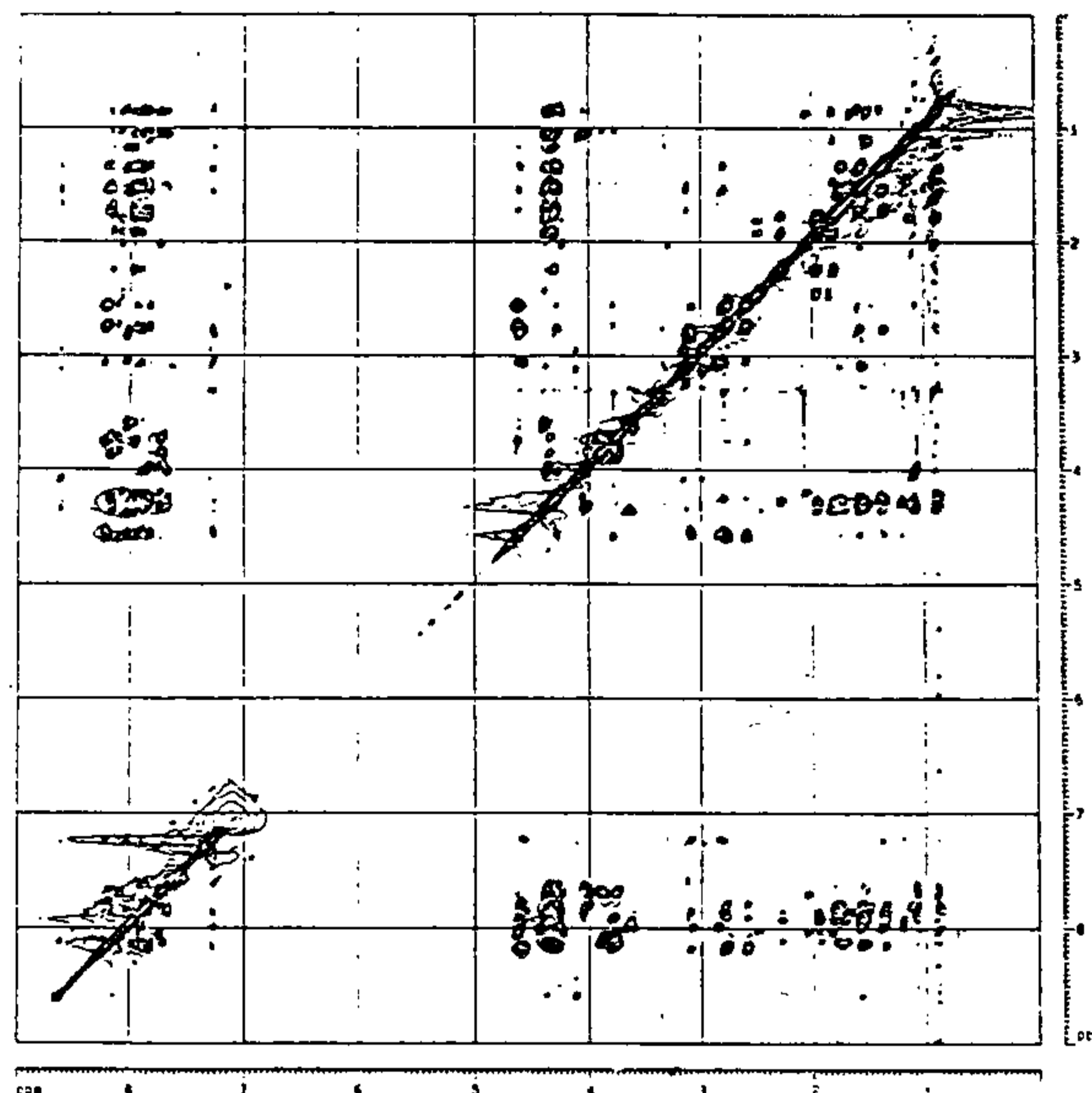


Figure 11 *a*. 600 MHz phase sensitive NOESY spectrum of the peptide 1-1-1 in DMSO at 40°C with a mixing time of 400 ms.

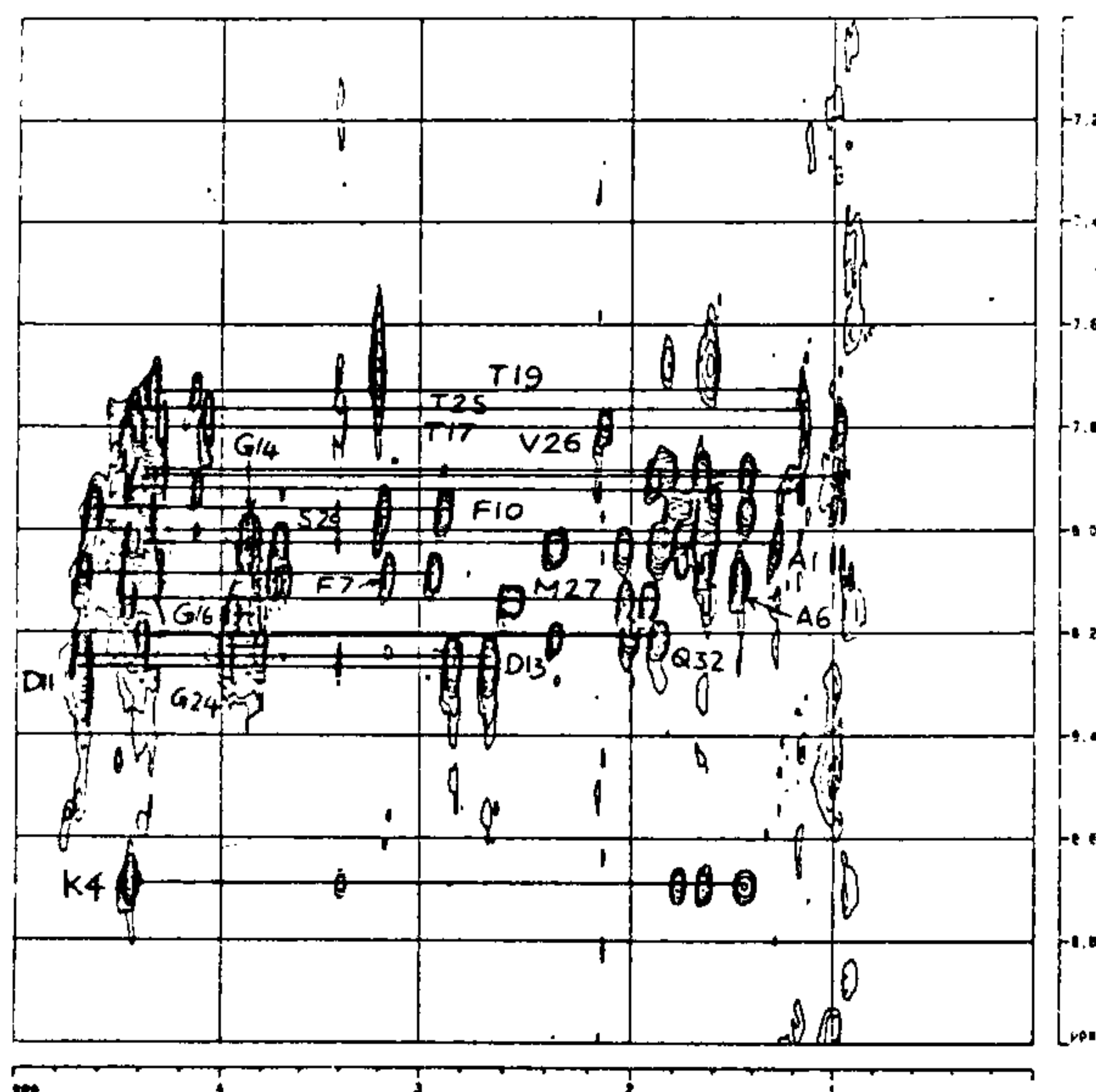


Figure 10 *b*. 600 MHz phase sensitive TOCSY spectrum of the peptide 1-1-1 in DMSO at 40°C with spin lock duration of 60 ms, showing a part of the TOCSY spectrum. Some of the coupling networks have been labelled.

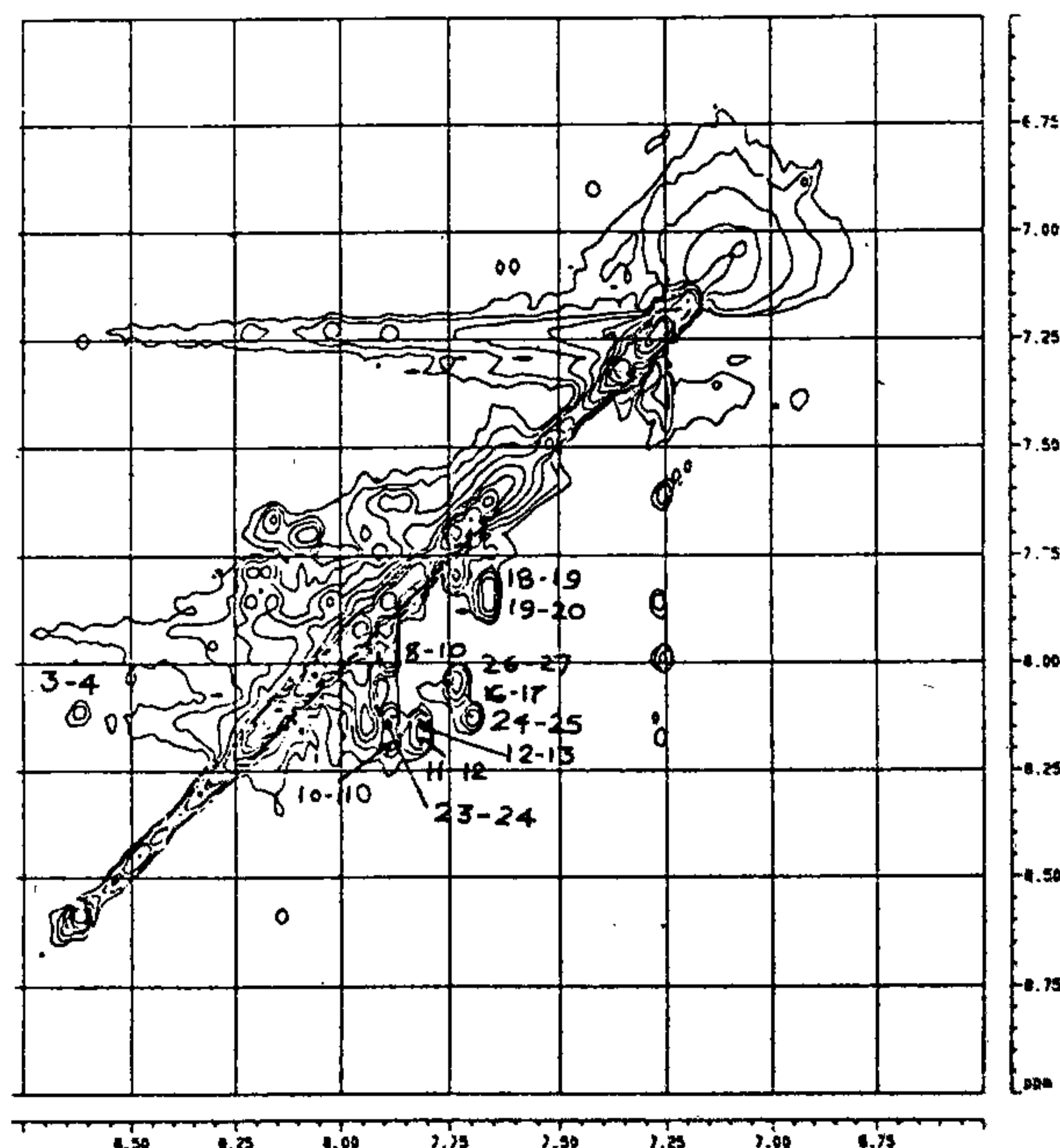


Figure 11 *b*. The amide region of the NOESY spectrum of the peptide 1-1-1.

Leu-23 and Gly-24. The unambiguous assignment of the two lysines, at sequence positions 4 and 12 enables the assignment of the remaining one to Lys-21. The presence of weak NH–NH cross peak between Lys-21 and another long side chain containing residue, helps in the assignment of Glu-22. Identification of the Leu-9 and Leu-23, made the assignment of the remaining leucine residue to Leu-30. A summary of through space connectivities inferred from 2D NOESY for the peptide 1–1–1 is given in Figure 12.

**Secondary structural elements.** The presence of strong NH–NH connectivities from the Phe-10 to Asp-15 and Gly-16 to Thr-20 indicates that the peptide exhibits helical structure in these regions. The NH resonance of all the three aspartates appears almost close to each other, making the assignment of the  $\alpha\text{CH}_i\text{--NH}_{i+3}$  cross peaks between the residues, Asp-11–Gly-14; Lys-12–Asp-15; and Asp-13–Gly-16, difficult. The absence of  $\alpha\text{CH}_i\text{--NH}_{i+3}$  for the peptide segment Gly-16 to Thr-20, indicates that this part is characterized by a loose helical segment. The strong  $\alpha\text{CH}_i\text{--NH}_{i+1}$  and a weak  $\alpha\text{CH}_i\text{--}\alpha\text{CH}_{i+1}$  between Asp-11 and Asp-15 indicate the possibility of an extended structure. Careful analysis of the  $\alpha\text{--}\alpha$  region shows only three distinct binary connectivities among residues 14–15, 24–25 and 8–9. In view of this lack of contiguous connectivity it is clear that the system, although may exist transiently as an anti-parallel  $\beta$ -sheet, the average conformation is more like an extended structure. All these point to a possible conformational equilibrium between an extended and

helical structure. This fact is again supported by the presence of weak sequential  $\alpha\text{CH}_i\text{--}\alpha\text{CH}_{i+1}$  connectivities for the residues Lys-12 to Asp-15. The presence of strong  $\alpha\text{CH}_i\text{--NH}_{i+1}$  and  $\text{NH}_i\text{--NH}_{i+1}$  cross peaks between the residues Phe-3–Lys-4; Gly-24–Thr-25; and Val-26–Met-27 indicates the possibility of a turn structure. The presence of  $\text{NH}_i\text{--NH}_{i+2}$  and  $\beta\text{CH}_i\text{--NH}_{i+2}$  connectivities between the residues Phe-7 and Phe-10 indicates the existence of a  $\beta$ -turn structure in this region. The end residues are not well characterized due to lack of NOE information.

## Summary and conclusions

A brief summary of the approach to the elucidation of 3D structure of fair-sized peptides using high resolution 2D NMR techniques has been presented and the procedure is illustrated with a small 32-residue peptide corresponding to the first calcium-binding domain of the protein calmodulin. Whereas this part in the crystal of the native molecule has a clear cut helix–loop–helix (EF motif) configuration, fragmentation has led to a large reduction in the secondary structure. It is unfortunate that the solubility of the fragment has been so low that the experiments had to be carried out in DMSO solution. Often NMR methods are supplemented with other experimental techniques such as circular dichroism, Fourier far IR and Raman spectroscopy. The results obtained are used as input into molecular modelling and molecular dynamics calculations<sup>19–23</sup> where the NMR NOEs can be used to provide certain constraints in

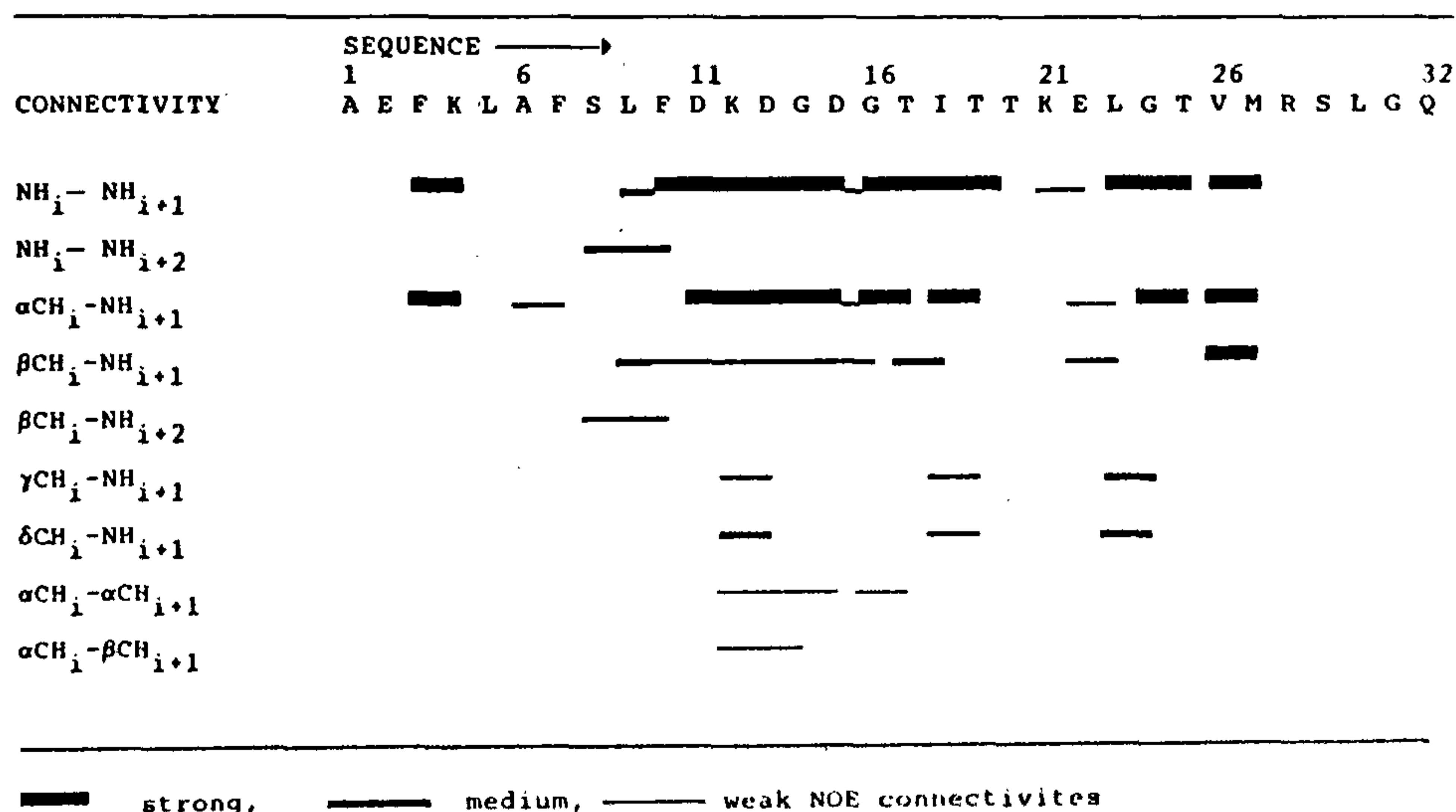


Figure 12. Schematic diagram showing the various through space connectivities derived from NOE data for the peptide 1–1–1.

interatomic distances so as to arrive at plausible structure in an expeditious way. Caution has to be exercised in using the NOE data when one suspects rapid interconversion between conformers.

1. Surewicz, W. K. and Mantsch, H. H., *Biochim. Biophys. Acta*, 1988, **952**, 115-130.
2. Ellis, G., Hendra, P. J., Hodges, C. M., Willis, H. A., Jawahari, T., Jones, C. H., Le Barazer, P., Passingham, C., Royaud, I. A. M., Sanchez-Blasquez, A. and Warnes, G. M., *The Analyst*, 1989, **114**, 1061.
3. Dyson, H. J. and Wright, P. E., *Ann. Rev. Biophys. Biophys. Chem.*, 1991, **20**, 519-538.
4. Yang, J.-T., Wu, C.-S. C. and Martinez, H. M., *Methods Enzymol.*, 1986, **130**, 208.
5. Wüthrich, K., *NMR of Proteins and Nucleic Acids*, J. Wiley, New York, 1986.
6. Marion, D., *NMR: Basic Principles and Progress* (eds Diehl, P., Fluck, E., Günther, H., Kosfeld, R. and Seelig, J.), Springer-Verlag, Berlin, 1991, vol. 25, pp. 91.
7. Bertini, I., Molinari, H. and Niccolai, N., in *NMR and Biomolecular Structure*, VCH, Weinheim, 1991.
8. Oppenheimer, N. J. and James, T. L., *Methods Enzymol.*, 1989, **176**.
9. Wagner, G., *Progr. NMR Spectrosc.*, 1990, **22**, 101; Wüthrich, K., *J. Biol. Chem.*, 1990, **265**, 22059-22062.
10. Lauterbur, P. C., *Nature*, 1973, **242**, 190.
11. Montford, C. E., Holmes, K. T. and Smith, I. C. P., in *Progress in Clinical Biochemistry and Medicine*, Springer-Verlag, Berlin, 1986, vol. 3.
12. Gadian, D. G., *Nuclear Magnetic Resonance and its Applications to Living Systems*, Clarendon, Oxford, 1982.
13. de Certaines, J. D., *Magnetic Resonance Spectroscopy of Biofluids*, World Scientific, Singapore, 1989.
14. Wagner, G., Braun, Havel, W. T. F., Schaumann, T., Go, N. and Wüthrich, K., *J. Mol. Biol.*, 1987, **196**, 611-639.
15. Nilges, M., Gronenborn, A. M., Brünger, A. T. and Clore, G. M., *Protein Eng.*, 1988, **2**, 27-38.
16. Wüthrich, K., *Science*, 1989, **243**, 45-50.
17. Schultze, P., Wörgötter, E., Braun, W., Wagner, G., Vašák, M., Kägi, J. H. R. and Wüthrich, K., *J. Mol. Biol.*, 1988, **203**, 251-268.
18. Klevit, R. E. and Waygood, E. B., *Biochemistry*, 1986, **25**, 7774-7781.
19. Havel, T. F., *DISGEO, QCPE*, 1986, No. 507, Indiana University.
20. Brooks, B. R., Brucoleri, R. E., Olafson, B. D., States, D. J., Swaminathan, S. and Karplus, M., *J. Comp. Chem.*, 1983, **4**, 187-217.
21. Weiner, S. J., Kollman, P. A., Case, D. A., Singh, U. C., Ghio, C., Alagona, G. and Profeta Jr. S. and Weiner, P., *J. Am. Chem. Soc.*, 1984, **106**, 765-784.
22. van Gunsteren, W. F. and Berendsen, H. J. C., *Biochem. Soc. Trans.*, 1982, **10**, 301.
23. Braun, W. and Go, N., *J. Mol. Biol.*, 1985, **186**, 611-626.
24. Dyson, H. J., Merutka, G., Waltho, J. P., Lerner, R. A. and Wright, P. E., *J. Mol. Biol.*, 1992, **226**, 795-817.
25. Dyson, H. J., Sayre, J. R., Merutka, G., Shin, H. C., Lerner, R. A. and Wright, P. E., *J. Mol. Biol.*, 1992, **226**, 819-835.
26. Alonso, D. O. V., Dill, K. A. and Stigter, D., *Biopolymers*, 1991, **31**, 1631-1649.
27. Neri, D., Billeter, M., Wider, G. and Wüthrich, K., *Proc. Natl. Acad. Sci. USA*, 1992, **89**, 4397.
28. Davis, G. D. and Tosteson, D. C., *Biochemistry*, 1975, **14**, 3962-3969.
29. Patel, D. J., *Biochemistry*, 1974, **13**, 2388-2395.
30. Lewin, B., *Genes V*, Oxford University Press, Oxford, 1994.
31. Hoppe, W., Lohmann, W., Markl, H. and Ziegler, H. (eds), *Biophysics*, Springer-Verlag, Berlin, 1982.
32. Ernst, R. R., Bodenhausen, G. and Wokaun, A., *Principles of Nuclear Magnetic Resonance in One and Two Dimensions*, Clarendon Press, Oxford, 1987.
33. Chandrakumar, N. and Subramanian, S., *Modern Techniques in High-Resolution FT-NMR*, Springer, New York, 1987.
34. Carlson, R. M. and Croasmun, W. R. (eds), *Methods Stereochem. Anal.*, 1987, **9**.
35. Griesinger, C., Sørensen, O. W. and Ernst, R. R., *J. Magn. Reson.*, 1989, **84**, 14-63.
36. Kay, L. E., Marion, D. and Bax, A., *J. Magn. Reson.*, 1989, **84**, 72-84; Marion, D., Kay, L. E., Spark, S. W., Torchia, D. A. and Bax, A., *J. Am. Chem. Soc.*, 1989, **111**, 1515-1517.
37. Bonmatin, J. M., Genest, M., Petit, M. C., Gincel, E., Simorre, J. P., Cornet, B., Gallet, X., Caille, A., Labbe, H., Vovelle, F. and Ptak, M., *Biochimie*, 1992, **74**, 825-836.
38. Griffey, R. H. and Redfield, A. G., *Q. Rev. Biophys.*, 1987, **19**, 51-82.
39. Kainoshi, M. and Tsuji, T., *Biochemistry*, 1982, **21**, 6273-6279.
40. Jeener, J., *Ampere International Summer School*, Basko Polje, Yugoslavia, 1971.
41. Aue, W. P., Bartholdi, E. and Ernst, R. R., *J. Chem. Phys.*, 1976, **64**, 2229-2246.
42. Bax, A., *Two-Dimensional NMR in Liquids*, Delft University Press, Delft, 1982.
43. Braunschweiler, L. and Ernst, R. R., *J. Magn. Reson.*, 1983, **53**, 521-528.
44. Freeman, R. and Morris, G. A., *Bull. Magn. Reson.*, 1979, **1**, 5-26.
45. Kessler, H., Gehrke, M. and Griesinger, C., *Angew. Chem. Int. Ed. Engl.*, 1988, **27**, 490-536.
46. Sanders, J. K. M. and Hunter, B. K., *Modern Techniques in High Resolution FT-NMR*, University Press, Oxford, 1987.
47. Benn, R. and Gunther, H., *Angew. Chem. Int. Ed. Engl.*, 1983, **22**, 350-380.
48. Freeman, R., *Proc. R. Soc. London*, 1980, **A373**, 149-178.
49. Morris, G. A., *Magn. Reson. Chem.*, 1986, **24**, 371-403.
50. States, D. J., Haberkorn, R. A. and Ruben, D. J., *J. Magn. Reson.*, 1982, **48**, 286-292.
51. Sørensen, O. W., Eich, G. W., Levitt, M. H., Bodenhausen, G. and Ernst, R. R., *Progr. NMR Spectrosc.*, 1983, **16**, 163-192.
52. Rance, M., Sørensen, O. W., Bodenhausen, G., Wagner, G., Ernst, R. R. and Wüthrich, K., *Biochem. Biophys. Res. Commun.*, 1983, **117**, 479-485.
53. Ernst, R. R., Bodenhausen, G. and Wokaun, A., *Principles of Nuclear Magnetic Resonance in One and Two Dimensions*, Clarendon Press, Oxford, 1987, pp. 349.
54. Eich, G. W., Bodenhausen, G. and Ernst, R. R., *J. Am. Chem. Soc.*, 1982, **104**, 3731-3732.
55. Bolton, P. H. and Bodenhausen, G., *Chem. Phys. Lett.*, 1980, **69**, 185-189.
56. Braunschweiler, L. and Ernst, R. R., *J. Magn. Reson.*, 1983, **53**, 521-528.
57. Bax, A., Davies, D. G. and Sarkar, S. K., *J. Magn. Reson.*, 1985, **63**, 230-234.
58. Levitt, M. H., Freeman, R. and Frenkiel, T., *Adv. Magn. Reson.*, 1983, **11**.
59. Shaka, A. J., Keeler, J., Frenkiel, T. and Freeman, R., *J. Magn. Reson.*, 1983, **52**, 335-338.
60. Shaka, A. J., Keeler, J. and Freeman, R., *J. Magn. Reson.*, 1983, **53**, 313-340.
61. Levitt, M. H. and Freeman, R., *J. Magn. Reson.*, 1981, **43**, 502-507.
62. Chandrakumar, N. and Subramanian, S., *J. Magn. Reson.*, 1985, **62**, 346-349.
63. Solomon, I., *Phys. Rev.*, 1955, **99**, 559-565.
64. Overhauser, A. W., *Phys. Rev.*, 1953, **89**, 689; *ibid*, **92**, 411.
65. Noggle, J. H. and Schirmer, R. E., *The Nuclear Overhauser Effect: Chemical Applications*, Academic Press, New York, 1971.

66. Macura, S. and Ernst, R. R., *Mol. Phys.*, 1980, **41**, 95-117.
67. Neuhaus, D. and Williamson, M. P., *The Nuclear Overhauser Effect in Structural and Conformational Analysis*, VCH Publishers, New York, 1989.
68. Schulz, G. E. and Schirmer, R. H., *Principles of Protein Structure*, Springer, New York, 1979.
69. Clore, G. M., Gronenborn, A. M., Brünger, A. T. and Karplus, M., *FEBS Lett.*, 1987, **213**, 269-277; Havel, T. F. and Wüthrich, K., *J. Mol. Biol.*, 1985, **182**, 281-294.
70. Clore, G. M., Sukumaran, D. K., Nilges, M., Zarbock, J. and Gronenborn, A. M., *EMBO J.*, 1987, **6**, 529-537.
71. Billeter, M. and Braun, W. and Wüthrich, K., *J. Mol. Biol.*, 1982, **155**, 321-346.
72. Arseniev, A., Schultze, P., Worgotter, E., Vasak, M., Kagi, J. H. R. and Wüthrich, K., *J. Mol. Biol.*, 1986, **187**, 131-135.
73. Karplus, M., *J. Am. Chem. Soc.*, 1963, **85**, 2870-2871.
74. Bystrov, V. F., *Prog. Nucl. Magn. Reson. Spectrosc.*, 1976, **10**, 41-81.
75. Nehaus, D., Wagner, G., Vašák, M., Kägi, J. H. R. and Wüthrich, K., *Eur. J. Biochem.*, 1985, **151**, 257-273.
76. Englander, S. W. and Wand, A. J., *Biochemistry*, 1987, **26**, 5953-5958.
77. Di Stefano, D. L. and Wand, A. J., *Biochemistry*, 1987, **26**, 7272-7281.
78. Piantini, U., Sørensen, O. W. and Ernst, R. R., *J. Am. Chem. Soc.*, 1982, **104**, 6800-6801.
79. Pardi, A., Wagner, G. and Wüthrich, K., *Eur. J. Biochem.*, 1983, **137**, 445-454.
80. Case, D. A., Dyson, H. J. and Wright, P. E., *Methods Enzymol.*, 1994, **239**, 392-416.
81. Bothner-By, A. A., Stephens, R. L., Lee, J., Warren, C. D. and Jeanloc, R. W., *J. Am. Chem. Soc.*, 1984, **106**, 811.
82. Bax, A. and Davis, D. G., *J. Magn. Reson.*, 1985, **63**, 207-213.
83. Markeley, J. L., Putter, I. and Jaretsky, O., *Science*, 1986, **161**, 6816.
84. Kalbitzer, H. R., Leberman, R. and Witingghofer, A., *FEBS Lett.*, 1985, **180**, 40.
85. Torchia, D. A., Sparks, S. W. and Bax, A., *Biochemistry*, 1988, **27**, 5135-5141.
86. Gomathi, L., Fairwell, T., Krishna, G. A., Ferretti, J. A. and Subramanian, S., *Curr. Sci.*, 1996, **70**, 910-927.
87. Merrifield, R. B., *Adv. Enzymol.*, 1969, **32**, 221.
88. Williamson, M. P. and Waltho, J. P., *Chem. Soc. Rev.*, 1992, 227-236.

ACKNOWLEDGEMENTS. We thank Thomas Fairwell, NHLBI, NIH, Bethesda, USA for providing the synthetic calmodulin fragments and Gopal A. Krishna, NHLBI, NIH, Bethesda, USA for a summer fellowship at NIH to L.G. Thanks are also due to James A. Ferretti of NHLBI, NIH, Bethesda, USA for providing 600 MHz NMR spectrometer. L.G. thanks the Indian Institute of Technology, Madras, for a fellowship.

Received 2 April 1996; revised accepted 22 August 1996

## All India Institute of Medical Sciences Ansari Nagar, New Delhi 110 029

### Training in Electron Microscopy for (1) Laboratory/Technical Staff and (2) Scientific Investigators

Two training programmes in Electron Microscopy (Biomedical Sciences) will be held for the 2 above mentioned categories of personnel during 1996-1997.

**Category I:** Laboratory/Technical Personnel: 26 Nov. to 10 Dec. 1996 (15 days);

**Category II:** Scientific Investigators: 6 Jan. to 27 Jan. 1997 (21 days).

#### **Eligibility**

**Category I:** B Sc degree and/or Diploma in MLT with minimum of 2 years experience in light microscopy. Number of seats are limited. Fee Rs 1000.

**Category II:** Ph D/MD or M Sc degree with 2-3 years of research experience. The applicant should state clearly the nature of the research project in which he/she is involved (in 200 words) and why training in Electron Microscopy is necessary for pursuing further research. Number of seats are limited. Fee Rs 3000.

Application on plain paper giving the following: (1) Name, (2) Age, (3) Postal address (fax number, if available may be indicated), (4) Sex, (5) Educational qualification, (6) Name of the University/Institution, (7) Year of passing, (8) Marks obtained, (9) Position(s) held, (10) Whether permanent/temporary, and (11) Letter of recommendation from the present employer, should reach Dr A. K. Susheela, Officer-in-Charge, Electron Microscope Facility, Department of Anatomy, AIIMS, New Delhi 110 029 (Fax: 686 2663) latest by 5 November 1996.

Selected candidates will be informed latest by 11 November 1996, when the Course fee should be remitted. Details will be provided in the Selection Letter.